Table 6. Sex differences in skin diseases

	Total; Male; Female		Total; Male; Female
Burn	892, 1.33%; 414, 1.34%; 478, 1.32%	Miscellaneous viral disorders	349, 0.52%; 171, 0.55%; 178, 0.49%
Trauma	406, 0.61%; 196, 0.63%; 210, 0.58%	Syphilis	24, 0.04%; 16, 0.05%; 8, 0.02%
Skin ulcer (nondiabetic)	1318, 1.97%; 605, 1.96%; 713; 1.97%	Miscellaneous sexually transmitted diseases	40, 0.06%; 26, 0.08%, 14, 0.04%
Pressure ulcer	606, 0.9%; 313, 1.01%; 293, 0.81%		
Miscellaneous physico-chemical skin damage	675, 1.01%; 303, 0.98%; 372, 1.03%	Bullous pemphigid	509, 0.76%; 208, 0.67%; 301, 0.83%
		Pemphigus	416, 0.62%; 180, 0.58%; 236, 0.65%
Diabetic dermatoses	432, 0.64%; 300, 0.97%; 132, 0.37%	Miscellaneous bullous diseases	139, 0.21%; 67, 0.22%; 72, 0.2%
Atopic dermatitis	6707, 10.01%; 3486, 11.28%; 3221, 8.92%	Systemic sclerosis	609, 0.91%; 94, 0.3%; 515, 1.43%
Hand eczema	2009, 3%; 532, 1.72%; 1477, 4.09%	Systemic lupus erythematosus	520, 0.78%; 72, 0.23%; 448, 1.24%
Contact dermatitis	2629, 3.92%; 902, 2.92%; 1727, 4.78%	Dermatomyositis	300, 0.45%; 76, 0.25%; 224, 0.62%
Seborrheic dermatitis	2201, 3.28%; 1295, 4.19%; 906, 2.51%	Miscellaneous collagen diseases	911, 1.36%; 209, 0.68%; 702, 1.94%
Miscellaneous eczema	12523, 18.68%; 6289, 20.35%, 6234, 17.26%	Anaphylactoid purpura	169, 0.25%; 72, 0.23%; 97, 0.27%
Urticaria/angioedema	3355, 5.01%; 1251, 4.05%; 2104, 5.82%	Reticular/racemous livedo	80, 0.12%; 21, 0.07%; 59, 0.16%
Prurigo	1216, 1.81%; 755, 2.44%; 461, 1.28%	Miscellaneous vasculitis/purpura/ circulatory disturbance	625, 0.93%; 239, 0.77%; 386, 1.07%
Drug eruption/toxicoderma	1012, 1.51%; 436, 1.41%; 576, 1.59%		
Psoriasis	2967, 4.43%; 2138, 6.92%; 829, 2.29%	Mycosis fungoides	418, 0.62%; 244, 0.79%; 174, 0.48%
Palmoplantar pustulosis	828, 1.24%; 284, 0.92%; 544, 1.51%	Miscellaneous lymphomas	283, 0.42%; 149, 0.48%; 134, 0.37%
Miscellaneous pustulosis	170, 0.255%; 67, 0.22%; 103, 0.29%	Pigmented nevus	703, 1.05%; 206, 0.67%; 497, 1.38%
Lichen planus	200, 0.3%; 80, 0.26%; 120, 0.33%	Seborrheic keratosis	1090, 1.63%; 537, 1.74%; 553, 1.53%
Miscellaneous inflammatory keratotic disorders	241, 0.36%; 95, 0.31%; 146, 0.4%	Soft fibroma/achrochordon	228, 0.34%; 78, 0.25%; 150, 0.42%
		Epidermal cyst	1183, 1.77%; 713, 2.31%; 470, 1.3%
Tylosis/clavus	911, 1.36%; 292, 0.95%; 619, 1.71%	Lipoma	171, 0.26%; 92, 0.3%; 79, 0.22%
Ichthyosis	61, 0.09%, 31, 0.1%; 30, 0.08%	Dermatofibroma	110, 0.16%; 44, 0.14%, 66, 0.18%
Miscellaneous keratinization disorders	502, 0.75%; 192, 0.62%; 310, 0.86%	Miscellaneous benign skin tumors	1651, 2.46%; 673, 2.18%; 978, 2.71%
		Actinic keratosis	256, 0.38%; 129, 0.42%; 127, 0.35%
Ingrown nail	594, 0.89%; 197, 0.64%; 397, 1.1%	Basal cell carcinoma	324, 0.48%; 166, 0.54%; 158, 0.44%
Miscellaneous nail disorder	396, 0.59%; 123, 0.4%; 273, 0.76%	Squamous cell carcinoma/Bowen's disease	447, 0.67%; 272, 0.88%; 175, 0.48%
Alopecia areata	1644, 2.45%; 557, 1.8%; 1087, 3.01%		
Androgenic alopecia	208, 0.31%; 198, 0.64%; 10, 0.03%	Paget's disease	221, 0.33%; 136, 0.44%; 85, 0.24%
Miscellaneous skin appendage disorders	266, 0.4%, 77, 0.25%; 189, 0.52%	Malignant melanoma	802, 1.2%; 395, 1.28%; 407, 1.13%
		Miscellaneous malignant skin tumors	531, 0.79%; 291, 0.94%; 240, 0.66%
Scabies	96, 0.14%; 50, 0.16%; 46, 0.13%	Vitiligo vulgaris	1123, 1.68%; 473, 1.53%; 650, 1.8%
Insect bite	762, 1.14%; 285, 0.92%; 477, 1.32%	Chloasma/senile freckle	334, 0.5%; 18, 0.06%; 316, 0.87%
Tinea pedis	4363, 6.51%; 2225, 7.2%; 2138, 5.92%	Miscellaneous pigmented disorders	154, 0.23%; 30, 0.1%; 124, 0.34%
Tinea unguium	3216, 4.8%; 1581, 5.12%; 1635, 4.53%	Erythema multiforme	194, 0.29%; 89, 0.29%; 105, 0.29%
Miscellaneous tinea	607, 0.91%; 404, 1.31%; 203, 0.56%	Erythema nodosum	111, 0.17%; 12, 0.04%; 99, 0.27%
Candidiasis	406, 0.61%; 176, 0.57%; 230, 0.64%	Miscellaneous disorders with erythematous plaques	130, 0.19%; 40, 0.13%; 90, 0.25%
Miscellaneous mycosis	209, 0.31%; 117, 0.38%; 92, 0.25%		
Acne	2423, 3.62%; 757, 2.45%; 1666, 4.61%	Nevus/phacomatosis (other than pigmented nevus)	266, 0.4%; 89, 0.29%; 177, 0.49%
Impetigo contagiosum	505, 0.75%; 283, 0.92%; 222, 0.61%		
Folliculitis	749, 1.12%; 432, 1.4%; 317, 0.88%	Rosacea/rosacea-like dermatitis	148, 0.22%; 36, 0.12%; 112, 0.31%
Erysipelas	81, 0.12%; 35, 0.11%; 46, 0.13%	Granulomatous diseases	192, 0.29%; 65, 0.21%; 127, 0.35%
Cellulitis	589, 0.88%; 304, 0.98%; 285, 0.79%	Keloid/hypertrophic scar	184, 0.27%; 73, 0.24%; 111, 0.31%
Miscellaneous bacterial infection	909, 1.36%; 497, 1.61%; 412, 1.14%	Cheilitis/angular cheilitis/mucous membrane diseases	94, 0.14%; 38, 0.12%; 56, 0.16%
Molluscum contagiosum	602, 0.9%; 327, 1.06%; 275, 0.76%		
Herpes simplex	688, 1.03%; 266, 0.86%; 422, 1.17%	Erythroderma	62, 0.09%; 44, 0.14%; 18, 0.05%
Herpes zoster/zoster-associated pain	1599, 2.39%; 694, 2.25%; 905, 2.51%	Other diseases	662, 0.99%; 315, 1.02%; 347, 0.96%
		Total	67 024, 100%; 30 899, 100%; 36 125, 100%
Viral wart	3016, 4.5%; 1388, 4.49%; 1628, 4.51%		

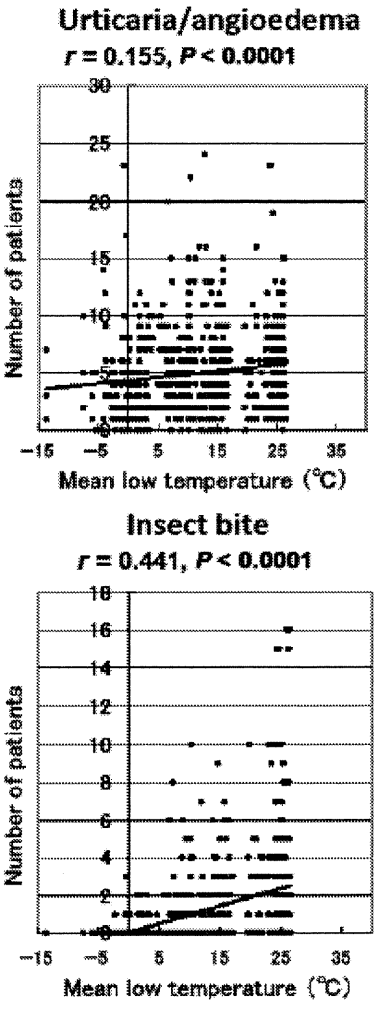

Figure 5. Correlation between patient numbers and mean low temperature in urticaria/angioedema and insect bite.

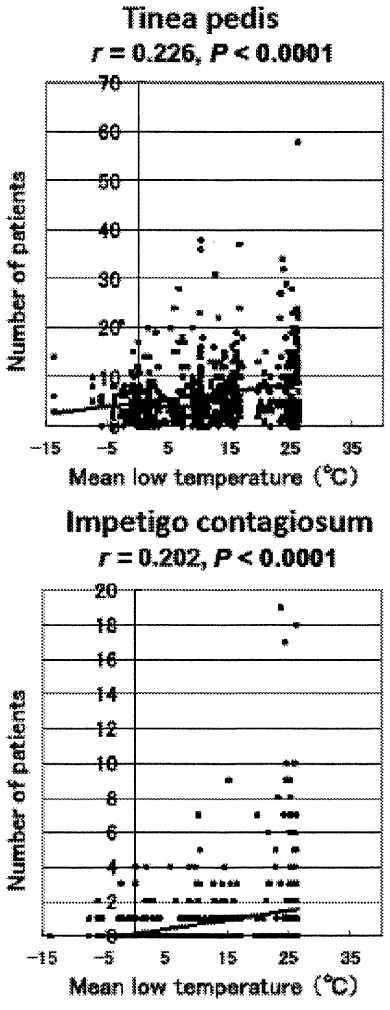

Figure 6. Correlation between patient numbers and mean low temperature in tinea pedis and impetigo contagiosum.

previous hospital-based study in Turkey[3] reported that the five most common disorders were atopic dermatitis, diaper dermatitis, impetigo, seborrheic dermatitis and miliaria in children aged 0–2 years; atopic dermatitis, impetigo, warts, contact dermatitis and insect bites in children aged 3–5 years; contact dermatitis, warts, atopic dermatitis, pruritus and impetigo in children aged 6–11 years; and acne, contact dermatitis, warts, seborrheic dermatitis and pruritus in children aged 12–16 years. For Dutch children aged 0–17 years old in 2001, the incidence rates per person-year of skin disorders were, in descending order, warts 34.3, dermatophytosis 25.4, contact dermatitis/other eczema 22.9, impetigo 20.5, laceration/cuts 20.3, atopic

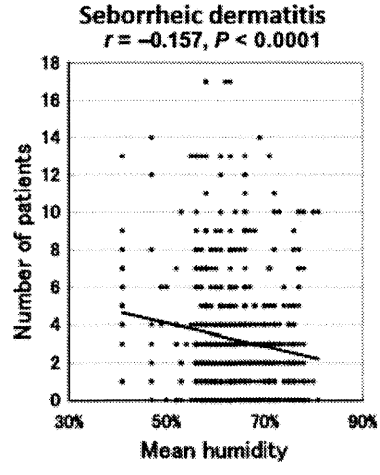

Figure 7. Negative correlation between patient numbers and mean humidity in seborrheic dermatitis.

dermatitis 16.5, moniliasis/candidasis 9.8 and molluscum contagiosum 9.5.[2] Although the order of each disease differed from country to country, atopic dermatitis, miscellaneous eczematous diseases, impetigo and warts appear to share their top rankings in pediatric dermatology, and this was also the case in Japan. Similar observations were also made in 1105 pediatric outpatients aged 0–15 years who visited the hospital of Aarau in Switzerland between 1998 and 2001.[7]

In Turkey, Yalçin *et al.*[8] examined records for 4099 geriatric patients over 65 years old who were admitted to the Ankara Numune Educational and Research Hospital from 1999 through 2003. The five most frequently diagnosed diseases were as follows: in the group aged 65–74 years, eczematous dermatitis, fungal infections, pruritus and bacterial and viral infections; in the group aged 75–84 years, eczematous dermatitis, pruritus, and fungal, viral and bacterial infections; and in the group aged over 85 years, pruritus, eczematous dermatitis, precancerous lesions and skin carcinomas, and viral and fungal infections.[8] In the present study, the Japanese geriatric population was also found to suffer very frequently from miscellaneous eczema and tinea pedis/unguium. In addition, there was a high incidence of psoriasis in elderly Japanese patients. As expected, we found conspicuous differences in the incidence of collagen diseases between the two sexes. A preponderance of collagen diseases in females was also evident in Yalçin's study.[8]

It should be emphasized again that this study was simply a measure of skin disorders in patients attending ordinary dermatology clinics in Japan. The study holds various limitations and biases, but it appears to highlight the current situation regarding patients presenting dermatological problems in Japan.

ACKNOWLEDGMENTS

We sincerely appreciate the considerable contribution and devotion of each clinic that participated in this study. The data management and statistical analysis was organized by EBMs Co., Ltd.

REFERENCES

1 Julian CG. Dermatology in general practice. *Br J Dermatol* 1999; **141**: 518–520.
2 Mohammedamin RS, van der Wouden JC, Koning S *et al.* Increasing incidence of skin disorders in children? A comparison between 1987 and 2001 *BMC Dermatol* 2006; **6**: 4.
3 Tamer E, Ilhan MN, Polat M, Lenk N, Alli N. Prevalence of skin diseases among pediatric patients in Turkey. *J Dermatol* 2008; **35**: 413–418.
4 Steer AC, Jenney AW, Kado J *et al.* High burden of impetigo and scabies in a tropical country. *PLoS Negl Trop Dis* 2009; **3**: e467.
5 Elliot AJ, Cross KW, Smith GE, Burgess IF, Fleming DM. The association between impetigo, insect bites and air temperature: a retrospective 5-year study (1999–2003) using morbidity data collected from a sentinel general practice network database. *Fam Pract* 2006; **23**: 490–496.
6 Rørtveit S, Rortveit G. Impetigo in epidemic and non-epidemic phases: an incidence study over 4 (1/2) years in a general population. *Br J Dermatol* 2007; **157**: 100–105.
7 Wenk C, Itin PH. Epidemiology of pediatric dermatology and allergology in the region of Aargau, Switzerland. *Pediatr Dermatol* 2003; **20**: 482–487.
8 Yalçin B, Tamer E, Toy GG, Oztaş P, Hayran M, Alli N. The prevalence of skin diseases in the elderly: analysis of 4099 geriatric patients. *Int J Dermatol* 2006; **45**: 672–676.

[7] Liao H, Waters AJ, Goudie DR, Aitken DA, Graham G, Smith FJ, et al. Filaggrin mutations are genetic modifying factors exacerbating X-linked ichthyosis. J Invest Dermatol 2007 Dec;127(12):2795–8.
[8] Smith FJ, Irvine AD, Terron-Kwiatkowski A, Sandilands A, Campbell LE, Zhao Y, et al. Loss-of-function mutations in the gene encoding filaggrin cause ichthyosis vulgaris. Nat Genet 2006 Mar;38(3):337–42.
[9] Elias PM, Crumrine D, Rassner U, Hachem JP, Menon GK, Man W, et al. Basis for abnormal desquamation and permeability barrier dysfunction in RXLI. J Invest Dermatol 2004 Feb;122(2):314–9.
[10] Flicek P, Amode MR, Barrell D, Beal K, Brent S, Chen Y, et al. Ensembl 2011. Nucleic Acids Res 2010;November.

Mårten C.G. Winge*
Dermatology Unit, Department of Medicine Solna, Karolinska Institutet, Karolinska University Hospital Solna, SE-171 76 Stockholm, Sweden

Torborg Hoppe
Department of Medical Sciences, Dermatology and Venereology, Uppsala University, SE-75185 Uppsala, Sweden

Agne Liedén
Magnus Nordenskjöld
Department of Molecular Medicine & Surgery, Karolinska Institutet, Karolinska University Hospital Solna, SE-171 76 Stockholm, Sweden

Anders Vahlquist
Department of Medical Sciences, Dermatology and Venereology, Uppsala University, SE-75185 Uppsala, Sweden

Carl-Fredrik Wahlgren
Dermatology Unit, Department of Medicine Solna, Karolinska Institutet, Karolinska University Hospital Solna, SE-171 76 Stockholm, Sweden

Hans Törmä
Department of Medical Sciences, Dermatology and Venereology, Uppsala University, SE-75185 Uppsala, Sweden

Maria Bradley[a,b]
[a]*Dermatology Unit, Department of Medicine Solna, Karolinska Institutet, Karolinska University Hospital Solna, SE-171 76 Stockholm, Sweden*
[b]*Department of Molecular Medicine & Surgery, Karolinska Institutet, Karolinska University Hospital Solna, SE-171 76 Stockholm, Sweden*

Berit Berne
Department of Medical Sciences, Dermatology and Venereology, Uppsala University, SE-75185 Uppsala, Sweden

*Corresponding author. Tel.: +46851776538
E-mail address: marten.winge@ki.se (M.C.G. Winge).

26 November 2010
10 March 2011
29 March 2011

doi:10.1016/j.jdermsci.2011.03.011

Letter to the Editor

Altered lipid profiles in the stratum corneum of Sjögren-Larsson syndrome

Sjögren-Larsson syndrome (SLS) is a rare, autosomal recessive neurocutaneous disorder characterized by clinical triads, congenital ichthyoids, spasticity and mental retardation [1]. SLS is caused by mutations in fatty aldehyde dehydrogenase (*FALDH*) (or *ALDH3A2*) gene [1]. FALDH is a microtonal NAD-dependent enzyme, which oxidizes medium- to long-chain aliphatic aldehydes to fatty acids. Accumulation of fatty alcohol has been shown in cultured fibroblasts and in plasma from SLS patients [1]. Numbers of mutations of *FALDH* gene have been shown, although only three mutations have been identified in Japanese SLS patients [2–4]. We here report a SLS patient who is a homozygote for one of the known mutations. In addition to assessing skin phenotype, permeability barrier function and cutaneous morphology, biochemical analysis revealed novel alterations in lipid profiles in the stratum corneum associated with barrier function.

A 57-year-old Japanese woman complaining of slightly pruritic and dry skin with scaling visited our hospital. The patient has been suffering from scaly skin lesions over the entire body since her early childhood. She presented generalized dryness, widespread itchy hyperkeratosis scaly lesions with brown scaling plaques, and slight erythema on the trunk and extremities (Fig. 1a). The neurologic examination revealed severe spastic paraplegia in the lower limbs with an increased muscle tone, hyperreflexia in all limbs, and positive Babinski reflexes bilaterally. She also showed mental retardation (IQ 39). A skin biopsy specimen from the right arm revealed orthohyperkeratosis with thin granular layers and mild acanthosis with papillomatosis (Fig. 1b). Electron microscopic examination showed several lipid droplets without surrounding membrane in the cornified cells (Fig. 1c). Moreover, abnormal lamellar granules, which lacked lamellar contents, were present in the granular cells (Fig. 1d). From these clinical features and cutaneous morphology, this patient was diagnosed as SLS. Mutation analysis using a cDNA sample from the patient's peripheral white blood cells showed a homozygous point mutation c.1157A>G which results in alteration from asparagine to serine at cordon 386 (p.Asn386Ser) in the β-9 chains containing active domain of FALDH (Fig. 2a).

Transepidermal water loss (TEWL) of the ichthyosiform lesion on the extensor and flexor sides of the forearm and back (6.3, 12.2, 10.2 g h^{-1} m^{-2}, respectively) was within the normal range (0–10, very good; 10–15, good; 15–20, fair; 25–30, poor; more than 30, very poor). On the other hand, water retention capability was impaired in the lesion (25.5, normal > 60).

Major barrier lipid content of involved skin was assessed in comparison to non-ichthyotic scaly lesions from sunburn dermatitis as a control subject (note: we and others found that there is no significant difference in lipid content of sunburn scale and of non-sunburn scales from normal donors [5]). Although there was no difference in the quantity of cholesterol between the patient and control, free fatty acid (FFA) was increased by about two-fold over control (Fig. 2b). In contrast, ceramide (Cer) 1, 6, 7 were decreased in the patient's scales compared with those in control samples, while membrane-bound Cer species, Cer A, which are constituent of the corneocyte lipid envelope (CLE), were increased. We recently demonstrated that linoleate required for acylceramide synthesis is primarily derived from triglyceride (TG) [6]. However, TG content was not changed in SLS compared with that in control scales (Fig. 2b).

The identical mutation in our case was described in another Japanese patient with SLS [2]. The other mutations reported in the

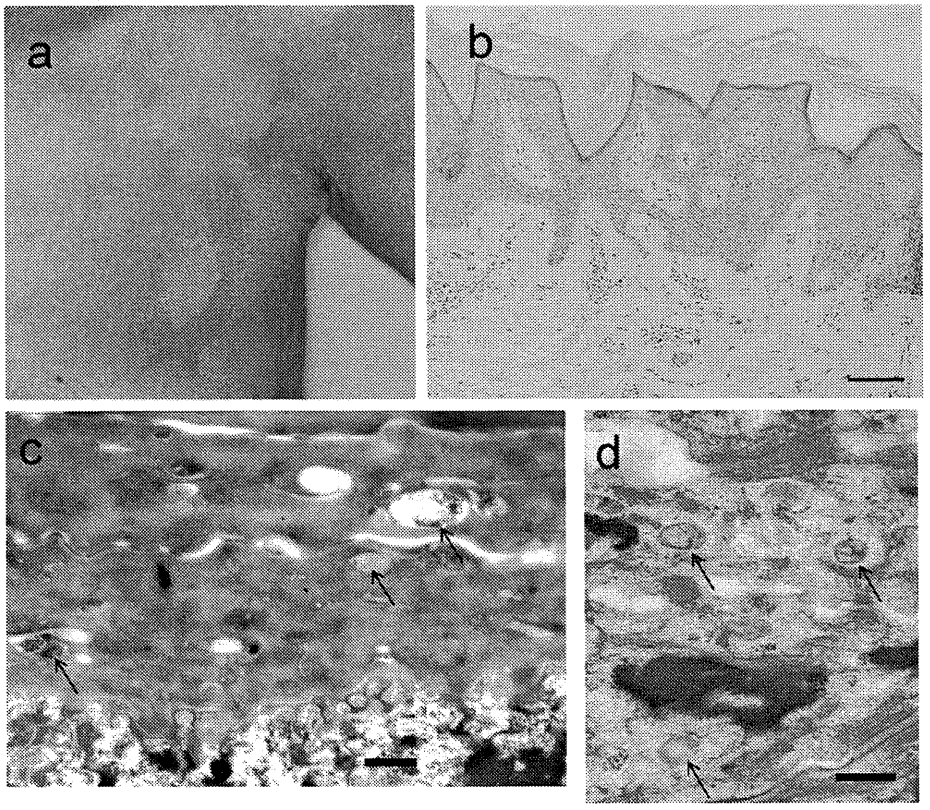

Fig. 1. Clinical appearance. (a) Scaly ichthyosiform erythema was apparent over the trunk. Morphological features of the patient's epidermis. (b) H&E staining of lesional skin from the patient's forearm. Orthohyperkeratosis, slightly thin granular layers and mild acanthosis with papillomatosis are noted, scale bar, 50 μm. (c) Ultrastructually, electron-lucent vacuoles are present within corneocytes (arrows) scale bar, 2 μm. (d) The presence of abnormal lamellar bodies lacking lamellar contents are evident in the cytoplasm of the granular cell (arrows) scale bar, 2 μm.

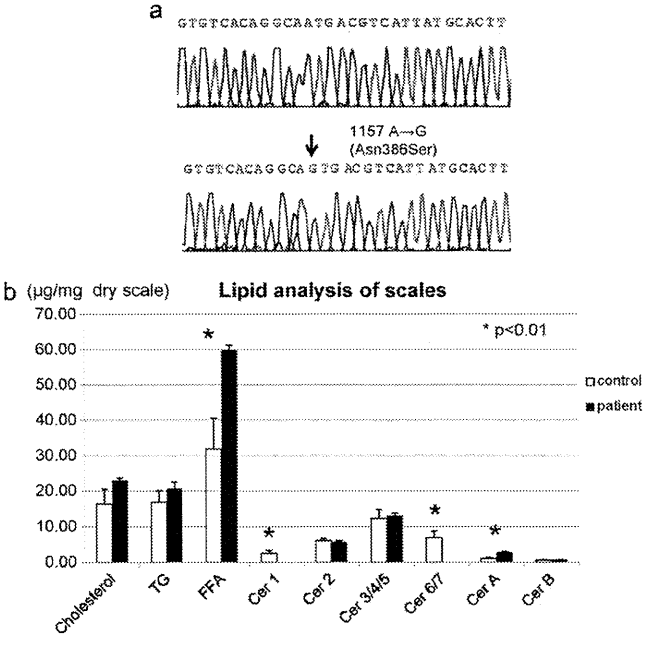

Fig. 2. (a) Sequencing analysis of FALDH gene. A homozygous point mutation (c.1157A>G) in the exon 8 that substitutes serine for asparagine at position 386 (p.Asn386Ser). (b) Lipid analysis of scales taken from sunburn lesions of a normal control individual (white bar) and from the patient's lesions (black bar) show increased FFA and Cer A level and decreased ceramide 1, 6, 7 levels in the patient's scale compared with control samples. Scales were taken from the upper back skin of the patient or control subjects. Gene and lipid analysis were performed as we described previously [4,6].

Japanese cases were c.481delA, c.1087_1089delGTA, c.332G>A (p.Trp111X) and c.636T>G (p.Ser212Arg) [3,4]. All the mutations found in Japanese families were distinct from one another and no founder effect was suggested in *ALDH3A2* mutations underlying Japanese SLS cases.

Recent studies by lanthanium perfusion assay, which is more sensitive for assessing permeability barrier function *in vitro* using skin sections than TEWL measurements employed in our study, reveals abnormal permeability barrier formation, structures, and function in SLS patients [7], while our present study is the first time for assessing both TEWL and hydration of SLS patient *in vivo*. Consistent with this prior study abnormal epidermal barrier structures [7] are evident in our patient, but alterations of TEWL were not observed. We assume that hyperkeratosis could attempt to compensate barrier dysfunction as previously suggested [8] and result in attempting to minimize barrier abnormality. Yet, decreased SC hydration in a SLS patient could alter normal SC environment, leading to abnormal epidermal homeostasis.

It remains to be resolved, however, why FFA level was high in spite of the deficient activity of FALDH, which was the enzyme catalyzing the sequential oxidation of fatty alcohol to fatty acid. It is likely that increased levels of wax esters and alkyl-diacylglycerol in scales and keratinocytes of SLS [9] derived from fatty alcohol may contribute to FFA production via hydrolysis with lipase, because the levels of these lipids were high.

Consistent with a prior study showing a deficiency of Cer 1, 6 in SLS patients' skin [10], Cer 1, 6, 7 were decreased in the epidermis of our case. We further demonstrated that the levels of CLE-bound ceramides, Cer A, which are produced from acylglucosylceramide, elevated in the scale from the patient, although Cer 1 (EOS) generated from the same precursors decreased. Therefore,

acylglucosylceramides appear to be preferentially utilized for CLE-bound ceramide production rather than free (CLE-unbound) lipid production in the SC. Exact mechanisms for CLE formation have not been elucidated yet and it remains to be resolved whether preferential utilization of acylglucosylceramide for CLE formation occurs only in the present case or also in other SLS patients. Moreover, it is unknown how decrease in Cer 1, 6, 7 occur and whether barrier lipid abnormality in the patient was a primary event or a secondary phenomenon in the pathogenesis of SLS skin lesions. Cer 1 is essential lipid species to form epidermal permeability barrier formation. Thus, not only accumulation of free fatty acids, but also deficiency of specific ceramide species might contribute to formation of ichthyotic phenotype in SLS.

Acknowledgements

We greatly thank Dr. Sumiko Hamanaka (Lab. for Molecular Membrane Neuroscience, RIKEN Brain Science Institute) and Dr. Ken Hashimoto (Department of Dermatology, Wayne State University School of Medicine) for helpful discussion.

References

[1] Rizzo WB, Carney G. Sjögren-Larsson syndrome: diversity of mutations and polymorphisms in the fatty aldehyde dehydrogenese gene (ALDH3A2). Hum Mutant 2005;26:1–10.
[2] Aoki N, Suzuki H, Ito K, Ito M. A novel point mutation of the *FALDH* gene in a Japanese family with Sjögren-Larsson syndrome. J Invest Dermatol 2000;114:1065–6.
[3] Shitake A, Akiyama M, Shimizu H. Novel ALDH3A2 heterozygous mutations are associated with defective lamellar granule formation in a Japanese family of Sjögren-Larsson syndrome. J Invest Dermatol 2004;123:1197–9.
[4] Sakai K, Akiyama M, Watanabe T, Sanayama K, Sugita K, Takahashi M, et al. Novel ALDH3A2 heterozygous mutations in a Japanese family with Sjögren-Larsson syndrome. J Invest Dermatol 2006;126:2545–7.
[5] Schreiner V, Gooris GS, Pfeiffer S, Lanzendörfer G, Wenck HW, Diembeck W, et al. Barrier characteristics of different human skin types investigated with X-ray diffraction, lipid analysis, and electron microscopy imaging. J Invest Dermatol 2000;114:654–60.
[6] Uhida Y, Cho Y, Moravian S, Kim J, Nakajima K, Crumbing D, et al. Neutral lipid storage leads to acylceramide deficiency, likely cobtributing to the pathogenesis of Dorfman-Chanarin syndrome. J Invest Dermatol 2010;130:2497–9.
[7] Rizzo WB, S'Aulis D, Jennings MA, Crumbing DA, Williams ML, Elias PM. Ichthyoisis in Sjögren-Larsson syndrome reflects defective barrier function due to abnormal lamellar body structure and secretion. Arch Dermatol Res 2010;302:443–51.
[8] Elias PM, Williams ML, Holleran WM, Jiang YJ, Schmuth M. Pathogenesis of permeability barrier abnormalities in the ichthyoses: inherited disorders of lipid metabolism. J Lipid Res 2008;49:694–714.
[9] Rizzo WB, Craft DA, Somer T, Carney G, Trafrova J, Simon M. Abnormal fatty alcohol metabolism in cultured keratinocytes from patients with Sjögren-Larsson syndrome. J Lipid Res 2008;49:410–9.
[10] Paige DG, Morse-Fisher N, Harper JI. Quantification of stratum corneum ceramides and lipid envelop ceramides in the hereditary ichthyoses. Br J Dermatol 1994;131:23–7.

Kimiko Nakajima*
Shigetoshi Sano
Department of Dermatology, Kochi Medical School, Kochi University, Nankoku, Japan

Yoshikazu Uchida
Department of Dermatology, School of Medicine, University of California San Francisco, CA, USA

Masashi Akiyama
Department of Dermatology, Nagoya University Graduate School of Medicine, Nagoya, Japan

Yukari Morita
Department of Geriatrics, Cardiology and Neurology, Kochi Medical School, Kochi University, Nankoku, Japan

Hiroshi Shimizu
Department of Dermatology, Hokkaido University Graduate School of Medicine, Sapporo, Japan

*Corresponding author. Tel.: +81 88 880 2363
E-mail address: nakajimk@kochi-u.ac.jp (K. Nakajima)

2 December 2010

doi:10.1016/j.jdermsci.2011.03.009

Letter to the Editor

BMP-4 down-regulates the expression of Ret in murine melanocyte precursors

Bone morphogenetic proteins (BMPs) have been implicated in a diverse array of biological processes including development and apoptosis [1]. Ret is involved in the physiological mechanisms of melanocyte activation and melanin production [2]. Ret expression in enteric neural precursors is initiated shortly after they emigrate from the neural plate.

We established three distinct cell populations of mouse neural crest (NC) cells, NCCmelb4, NCCmelb4M5 and NCCmelan5. NCCmelb4 cells have the potential to differentiate into mature melanocytes, but since they express melanocyte markers such as tyrosinase-related protein 1, DOPAchrome tautomerase and Kit, we consider them to be immature melanocytes, not multipotent precursors that can differentiate into neurons, as well as glia [3]. NCCmelb4M5 cells belong to the melanocyte lineage, but are less differentiated than NCCmelb4 cells [4]. NCCmelb4M5 cells do not express Kit and grow independently of the Kit ligand; these cells have the potential to differentiate into NCCmelb4 cells, which are Kit-positive melanocyte precursors. NCCmelan5 cells demonstrate the characteristics of differentiated melanocytes. We have also established an oncogene Ret-transgenic mouse line, line 304/B6, in which skin melanosis, benign melanocytic tumors and malignant melanomas develop in a stepwise fashion [2]. A malignant melanoma cell line, Mel-Ret, was established from the Ret-transgenic mouse. We found that all four cell lines express BMP receptors using Western blotting analysis (data not shown).

Western blotting revealed expression of the Ret protein in NCCmelb4M5 and in Mel-Ret cells, but in contrast, there was no expression of the Ret protein in NCCmelb4 or NCCmelan5 cells (Fig. 1A). Immunostaining also revealed that NCCmelb4M5 (Fig. 1B) and Mel-Ret cells are positive for Ret, but NCCmelb4 and NCCmelan5 cells are negative for Ret. Thus, Ret protein is expressed in most immature melanoblasts, while melanocytes are negative for Ret. We then analyzed Ret protein expression in BMP-4-treated NCCmelb4M5 cells by Western blotting (Fig. 1C–F). BMP-4 was added to the medium and incubated for 3 days at varying concentrations. After incubation with 10 ng/ml BMP-4 for 3 days, Ret protein expression was decreased, and disappeared completely

See related commentary on pg 1787

ORIGINAL ARTICLE

Consequences of Two Different Amino-Acid Substitutions at the Same Codon in *KRT14* Indicate Definitive Roles of Structural Distortion in Epidermolysis Bullosa Simplex Pathogenesis

Ken Natsuga[1], Wataru Nishie[1], Brian J. Smith[2,3], Satoru Shinkuma[1], Thomasin A. Smith[4], David A.D. Parry[4,5], Naoki Oiso[6], Akira Kawada[6], Kozo Yoneda[7], Masashi Akiyama[1,8] and Hiroshi Shimizu[1]

Numerous inherited diseases develop due to missense mutations, leading to an amino-acid substitution. Whether an amino-acid change is pathogenic depends on the level of deleterious effects caused by the amino-acid alteration. We show an example of different structural and phenotypic consequences caused by two individual amino-acid changes at the same position. Epidermolysis bullosa simplex (EBS) is a genodermatosis resulting from *KRT5* or *KRT14* mutations. Mutation analysis of an EBS family revealed that affected individuals were heterozygous for a, to our knowledge, previously unreported mutation of c.1237G>C (p.Ala413Pro) in *KRT14*. Interestingly, 2 of 100 unrelated normal controls were heterozygous, and 1 of the 100 was homozygous for a different mutation in this position, c.1237G>A (p.Ala413Thr). *In silico* modeling of the protein demonstrated deleterious structural effects from proline substitution but not from threonine substitution. *In vitro* transfection studies revealed a significantly larger number of keratin-clumped cells in HaCaT cells transfected with mutant *KRT14* complementary DNA (cDNA) harboring p.Ala413Pro than those transfected with wild-type *KRT14* cDNA or mutant *KRT14* cDNA harboring p.Ala413Thr. These results show that changes in two distinct amino acids at a locus are destined to elicit different phenotypes due to the degree of structural distortion resulting from the amino-acid alterations.

Journal of Investigative Dermatology (2011) **131,** 1869–1876; doi:10.1038/jid.2011.143; published online 19 May 2011

INTRODUCTION

Keratins are the largest group of intermediate filament proteins, which are expressed in epithelial cells (Schweizer *et al.*, 2006). The prominent intermediate filaments consist of keratins K1–K20, which are further classified into types I (K9–K20) and II (K1–K8). Type I and II keratins form non-covalent type I/II keratin heteropolymers (Moll *et al.*, 1982). Unique keratin expression serves as specific markers that characterize different epithelial cell types. Of the many kinds of epithelial cells that exist, basal epidermal keratinocytes preferentially express K5/K14 heteropolymers (Moll *et al.*, 1982; Nelson and Sun, 1983). These, in turn, form predominantly heterodimers *in vivo* (Coulombe and Fuchs, 1990; Hatzfeld and Weber, 1990; Steinert, 1990), with chains parallel to one another and in axial register (Conway and Parry, 1990; Steinert *et al.*, 1993).

Epidermolysis bullosa (EB) comprises a group of heterogeneous disorders in which congenital skin fragility leads to dermal–epidermal junction separation. EB has been subdivided into three major groups (EB simplex, junctional EB, and dystrophic EB) and one minor subtype (Kindler syndrome) based on the level of blister formation (Fine *et al.*, 2008). So far, mutations in 14 different genes have been identified as underlying EB subtypes (Fine *et al.*, 2008; Groves *et al.*, 2010). Among them, mutations in either the *KRT5* or *KRT14* gene, which encodes K5 and K14, respectively, lead to EB simplex (EBS) (Coulombe *et al.*, 1991; Lane *et al.*, 1992; Yasukawa *et al.*, 2006). According to the clinical severity of blister formation, EBS can be further subdivided into three major subtypes (Fine *et al.*, 2008). The mildest variant is "EBS, localized" (EBS-loc), with blistering confined to the

[1]*Department of Dermatology, Hokkaido University Graduate School of Medicine, Sapporo, Japan;* [2]*Walter and Eliza Hall Institute of Medical Research, Parkville, Victoria, Australia;* [3]*Department of Medical Biology, University of Melbourne, Parkville, Victoria, Australia;* [4]*Institute of Fundamental Sciences, Massey University, Palmerston North, New Zealand;* [5]*Riddet Institute, Massey University, Palmerston North, New Zealand;* [6]*Department of Dermatology, Kinki University Faculty of Medicine, Osaka, Japan;* [7]*Department of Dermatology, Kagawa University Faculty of Medicine, Kagawa, Japan and* [8]*Department of Dermatology, Nagoya University Graduate School of Medicine, Nagoya, Japan*

Correspondence: Ken Natsuga, Department of Dermatology, Hokkaido University Graduate School of Medicine, North 15 West 7, Sapporo 060-8638, Japan. E-mail: natsuga@med.hokudai.ac.jp

Abbreviations: cDNA, complementary DNA; EB, epidermolysis bullosa; EBS, EB simplex; MD, molecular dynamics; NHEK, normal human epidermal keratinocyte

Received 22 November 2010; revised 11 March 2011; accepted 26 March 2011; published online 19 May 2011

hands and feet; the more moderate variant is "EBS, other generalized" (EBS-gen-non-DM), with generalized blister formation; and the most severe variant is Dowling–Meara type (EBS-DM), which is characterized by severe herpetiform blistering (Fine *et al.*, 2008; Coulombe *et al.*, 2009).

In this study, we identified a, to our knowledge, previously unreported missense mutation in *KRT14* from a family with EBS-loc. We also detected a different nucleotide substitution at the same position in *KRT14* in normal control individuals. To clarify whether each nucleotide substitution is pathogenic, we used molecular modeling to predict the effect on the structure that results from a single amino-acid change, and we examined cultured cells transfected either with wild-type or with mutated *KRT14* complementary DNA (cDNA). Here, we show that two kinds of amino-acid changes at the same position of *KRT14* lead to totally different cell function *in vitro* and phenotypes *in vivo*.

RESULTS

Case description

The proband was a 10-year-old male with blistering on his soles (Figure 1a). Blisters on his hands and feet were observed during infancy. New blisters tended to emerge more in the summer. Nail deformity was also noted (Figure 1b). Ultrastructural features of skin specimens from the proband revealed many vacuoles scattered between the nucleus and basal lamina in the basal keratinocytes (Figure 1c). His family had several affected members (Figure 1d).

Detection of a novel *KRT14* mutation in a family with EBS and another nucleotide substitution at the same position of *KRT14* in normal controls

Direct sequencing of the *KRT5/KRT14* gene revealed that the proband (III-2, Figure 1d) was heterozygous for the, to our knowledge, previously unreported mutation of c.1237G>C transversion (p.Ala413Pro) in the helix termination motif of *KRT14* (Figure 2a). No other mutations were detected in any of the exons or exon–intron boundaries of *KRT5* and *KRT14*.

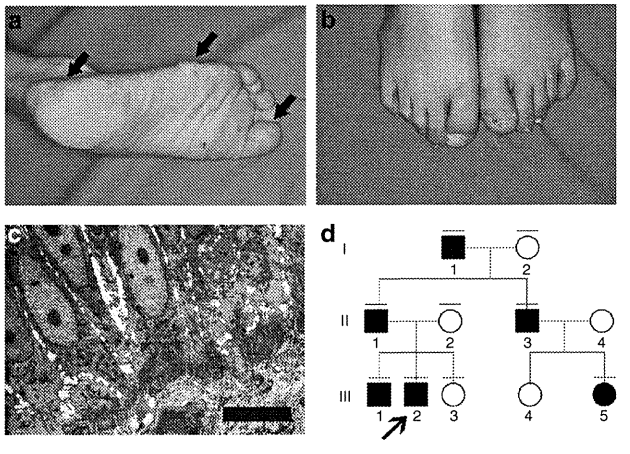

Figure 1. Clinical and ultrastructural features of a family with epidermolysis bullosa simplex. (**a**) Blisters and erosions are seen in the proband's right sole (arrows). (**b**) Toenail deformities are observed in the proband. (**c**) Ultrastructural features of the proband's lesional skin sample show basal cell cytolysis (bar = 5 μm). No apparent keratin clumps are seen. (**d**) Pedigree of the proband's family. Affected individuals are indicated by black fill. The proband is indicated by an arrow.

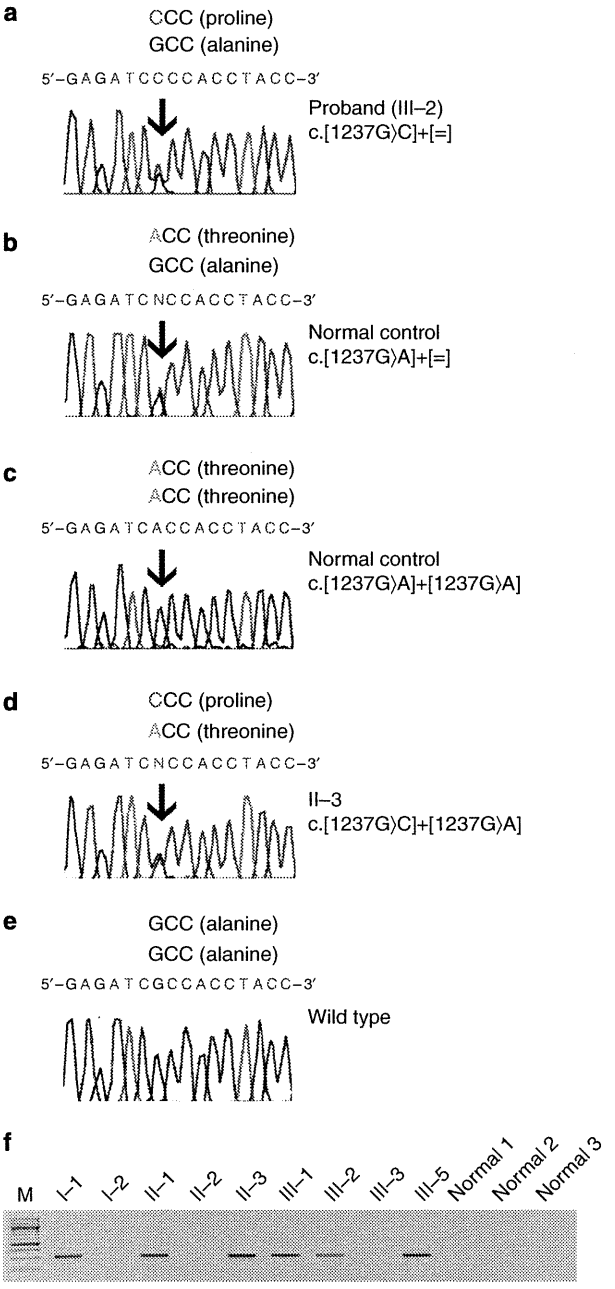

Figure 2. *KRT14* mutation analysis. (**a**) The proband (III-2) is heterozygous for c.1237G>C (p.Ala413Pro) in *KRT14* (an arrow). (**b**) In all, 2 out of 100 normal controls are heterozygous for c.1237G>A (p.Ala413Thr; an arrow). (**c**) Similarly, 1 out of 100 normal controls is homozygous for c.1237G>A (p.Ala413Thr; an arrow). (**d**) The proband's uncle (II-3) is compound heterozygous for c.1237G>C (p.Ala413Pro) and c.1237G>A (p.Ala413Thr; an arrow). (**e**) The wild-type sequence. (**f**) Mutant allele-specific amplification shows that affected family members (Figure 1d) harbor c.1237G>C (p.Ala413Pro).

Affected family members were also heterozygous for the same mutation in *KRT14* (I-1, II-1, II-3, III-1, and III-5; Figure 1d), and unaffected family members did not have that mutation (I-2, II-2, and III-3; Figure 1d). Mutant allele-specific amplification analysis demonstrated that a 300-bp fragment derived from the mutant allele was amplified from the genomic DNA of affected family members (Figures 1d and 2f). This mutation was not found in 200 normal unrelated alleles (100 Japanese individuals) by direct sequencing. Unexpectedly, 2 of the 100 normal Japanese controls were heterozygous for c.1237G>A transition (p.Ala413Thr) in *KRT14* (Figure 2b), and 1 of the 100 normal controls was homozygous for the same nucleotide transition (Figure 2c). These three individuals with the c.1237G>A transition (p.Ala413Thr) in *KRT14* had no history of skin fragility or nail dystrophy. Interestingly, the proband's unaffected grandmother (I-2) and affected uncle (II-3) were also heterozygous for the c.1237G>A transition (p.Ala413Thr) in *KRT14*. The proband's affected uncle (II-3) was compound heterozygous for p.Ala413Thr and p.Ala413Pro (Figure 2d). However, his clinical manifestations were similar to those of the other affected family members. The proband's unaffected cousin (III-4) is expected to be heterozygous for p.Ala413Thr—mutation analysis could not be performed without her consent.

Molecular dynamics predicts the deleterious structural change resulting from p.Ala413Pro substitution in keratin 14 but not from p.Ala413Thr

An initial structure of the native K5/K14 heterodimer and the p.Ala413Thr and p.Ala413Pro mutants, representing the C-terminal 35 residues of each chain, was generated by comparative modeling. The first 29 residues of each chain form a classical coiled coil in which generally hydrophobic residues occupy the heptad-repeat positions "*a*" and "*d*" (Figure 3a), a lysine at position 405 in K14 and 460 in K5, conserved among human intermediate filament proteins (Strelkov *et al.*, 2002), interact with each other through the hydrophobic portion of their side chains.

The structure of the native K5/K14 and the two mutants were subjected to molecular dynamics (MD) simulations to explore the structural stability. The secondary structure content in each of the chains throughout the MD simulations is presented in Figure 3b–d—in this figure, α-helix conformation is represented in blue. In this native heterodimer (Figure 3b), the α-helix content remains essentially unchanged throughout the simulation—both peptides maintain helical geometry across the coiled-coil domains (residues 449–474 in K5 and 394-419 in K14). At the C termini of K5 and K14, a stable bend (green), flanked on the N-terminal side by a stable short turn (yellow), is observed. In K5, a short 3_{10} helix (gray) forms after ~16 nanoseconds and is stable for the remainder of the simulation. Thus, the structure, and particularly the secondary structure conformation, remains constant throughout the simulation in the native complex.

The p.Ala413Thr mutation introduces a slight instability in the helix at the site of the mutation (black triangle), represented by an infrequent change in conformation to "turn" during the simulation (shown in yellow; Figure 3c). However, the overall α-helix content in this mutant is very similar to that observed for the native (Figure 3b). In contrast, in the p.Ala413Pro, peptide predominantly adopts a non-helical conformation at the position of the mutation throughout the simulation (Figure 3d). This change in conformation is also associated with additional instability (turn and coil conformation) in the helical conformation of residues C-terminal of the mutation site in both the K5 and K14 peptides (Figure 3d). Thus, the p.Ala413Thr mutation introduces a slight instability into the structure of the complex, whereas the p.Ala413Pro mutation causes significant disruption to the secondary structure in the C-terminal region of both peptides.

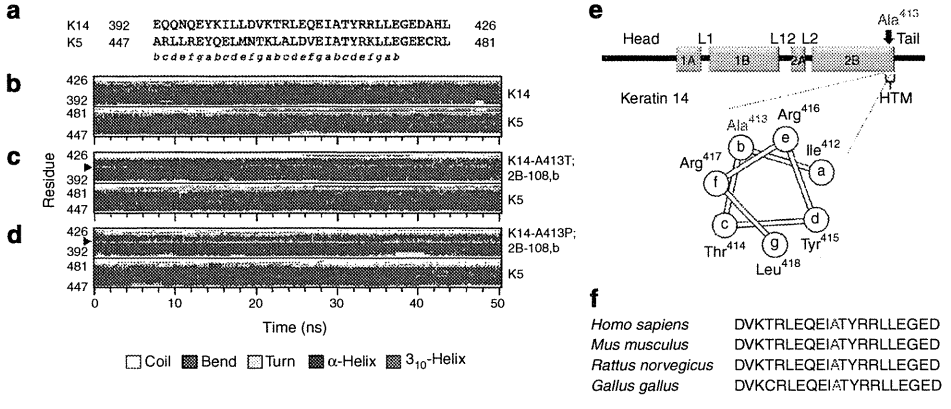

Figure 3. Molecular dynamics (MD) of the keratin heterodimer. (**a**) Sequences of the keratin helix motif and the heptad-repeat positions in K5 and K14. (**b–d**) MD simulations. The changes in secondary structure due to an amino-acid substitution were visualized through the MD. These simulations were each run for 50.0 nanoseconds. Blue indicates the α-helix. The native (**b**) and p.Ala413Thr (**c**) peptides retain α-helix geometry (blue colored) throughout the simulation. In contrast, increased instability in the α-helix was observed in the p.Ala413Pro-mutant peptide (**d**) bound with K5, which is indicated by the appearance of yellow-colored turn motif (arrowheads). In the p.Ala413Pro peptide (**d**), the helical geometry at the C terminus of both K14 and K5 is substantially compromised throughout the simulation—K5 is unstructured (coil geometry), and K14 alternates between coil, bends, and turns geometries. (**e**) A schematic diagram of K14 structure. Note that Ala^{413} is located at the helix termination motif (HTM) of the keratin molecule. Ala^{413} corresponds to position "*b*" of the heptad repeat (*abcdefg*) and is conserved among keratin polypeptides. (**f**) K14 amino-acid sequence alignment shows the level of conservation in diverse species of the amino acid Ala^{413} (red characters).

An alanine to proline substitution at the 413 locus of KRT14 protein disrupts the KIF network in HaCaT cells, whereas alanine to threonine does not

We examined whether the clinical heterogeneity between individuals with wild-type, p.Ala413Thr, and p.Ala413Pro mutations in *KRT14* could be demonstrated in a cell culture system. Three mammalian expression vectors containing the wild-type *KRT14* cDNA (K14WT), the mutated *KRT14* cDNA correspondent with the p.Ala413Thr substitution (K14A413T), and the p.Ala413Pro substitution (K14A413P) were transiently transfected into HaCaT cells. Detection of K14 was performed by probing the V5 epitope tag. Immunoblot analysis confirmed that each construct was successfully transferred into the HaCaT cells (Figure 4a).

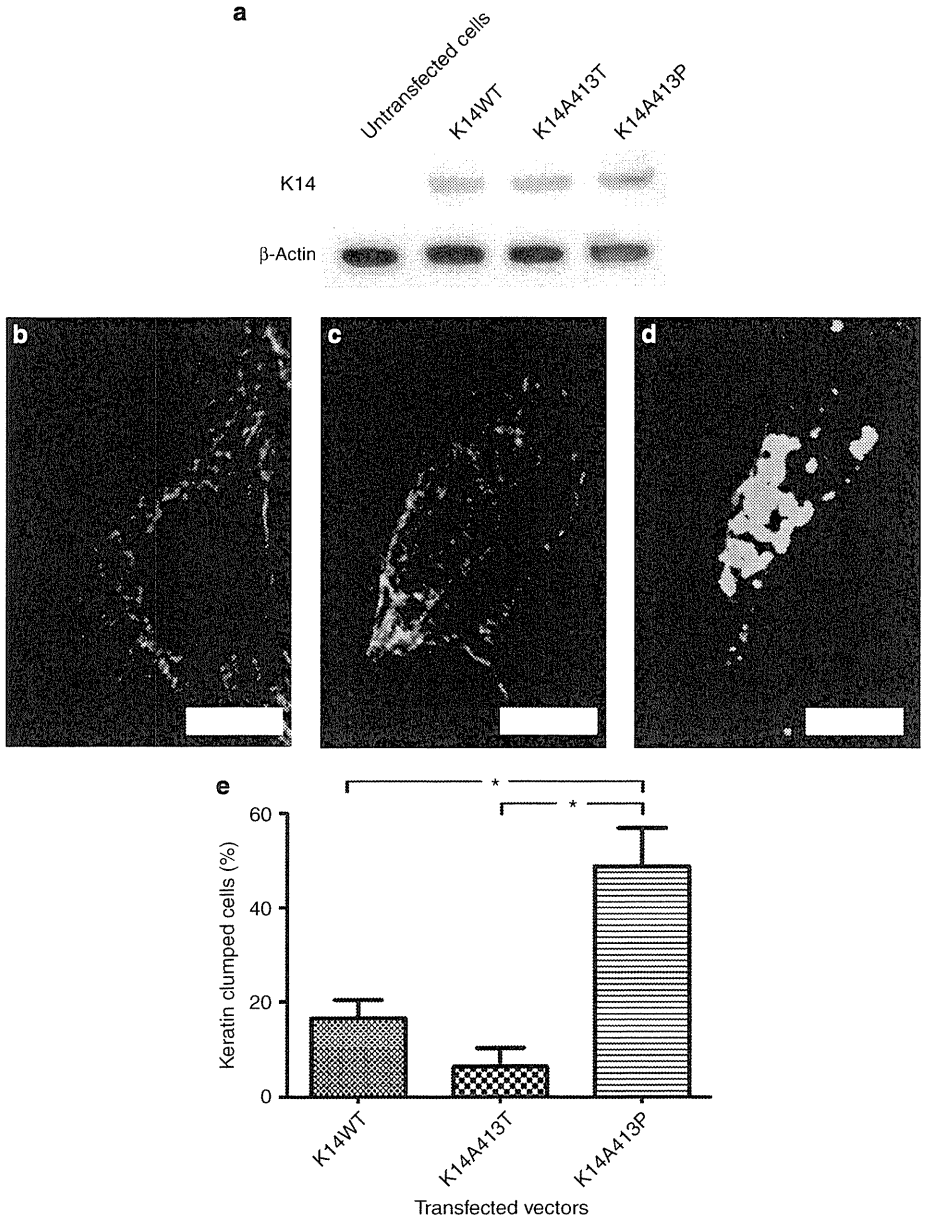

Figure 4. *In vitro* assay using HaCaT cells transfected with mutated *KRT14* complementary DNA (cDNA). (**a**) Immunoblot analysis reveals that HaCaT cells transfected with either wild-type (K14WT) or mutated *KRT14* cDNA (K14A413T and K14A413P) express V5-tagged K14 molecules. Equal protein loading was confirmed by reprobing with AC15 (anti-β-actin antibody). HaCaT cells transfected with K14WT (**b**), K14A413T (**c**), or K14A413P (**d**; bar = 5 μm). To visualize the transfected gene product, cells were stained with FITC-conjugated anti-V5 antibody. Cells transfected with K14WT and K14A413T have a normal keratin filament network (**b, c**), whereas significantly more cells transfected with K14A413P exhibit small ball-like clump formation (**d**). (**e**) The percentage of cells showing keratin aggregate formation among transfected cells is compared. There are significantly more clumps observed in the K14A413P-transfected cells (49 ± 8%) than in those transfected with either K14WT (17 ± 3%) or K14A413T (6 ± 4%). Each value shown represents the mean ± SEM of 10 individual samples. The statistical significance of the differences between groups is assessed by one-way analysis of variance, followed by Tukey's test (*$P<0.05$).

Transfection efficiency was up to 50% as judged from the immunofluorescence of the V5 epitope tag in transfected cells. The cells transfected with either K14WT or K14A413T showed fine bundles of keratin filaments extending throughout the cytoplasm without disturbing the cells' morphology (Figure 4b and c), whereas cells transfected with K14A413P exhibited small ball-like filament aggregates, indicating a disruption in the keratin network (Figure 4d). The percentage of the transfected cells harboring keratin clumping in each transfection assay was as follows: K14WT (mean, 17%), K14A413T (6%), and K14A413P (49%; Figure 4e). Statistical analysis showed that significantly more clumped cells were observed in HaCaT cells transfected with K14A413P than in those transfected with K14WT or K14A413T ($P<0.05$; Figure 4e).

Although not statistically significant ($P>0.05$), fewer keratin-clumped cells were observed in HaCaT cells transfected with K14A413T than those transfected with K14WT (Figure 4e). To clarify whether p.Ala413Thr mutation has a protective effect on keratin aggregation, three different transfections using HaCaT cells were performed, including K14A413P alone, a combination of equal amounts of K14A413P and K14A413T (K14A413P/K14A413T), and a combination of equal amounts of K14A413P and K14WT (K14A413P/K14WT). The percentage of the transfected cells harboring keratin clumping in each transfection assay was as follows: K14A413P (mean, 42%), K14A413P/K14A413T (32%), and K14A413P/K14WT (30%; Supplementary Figure S1 online). The differences in the percentage of keratin-clumped cells between K14A413P/K14A413T and K14A413P/K14WT were not statistically significant ($P>0.05$), indicating that the p.Ala413Thr mutation is unlikely to have a protective effect on keratin aggregation compared with the wild-type sequence.

We further performed three different transfections (K14WT, K14A413T, and K14A413P) into HeLa cells, in which endogenous K5 and K14 were not expressed but K8 was present as a potential partner of recombinant K14 (Hatzfeld and Franke, 1985; Albers and Fuchs, 1987). The percentage of the transfected cells harboring keratin aggregation in each transfection assay was as follows: K14WT (mean, 14%), K14A413T (10%), and K14A413P (77%; Supplementary Figure S2 online). Statistical analysis showed that significantly more clumped cells were observed in HeLa cells transfected with K14A413P than in those transfected with K14WT or K14A413T ($P<0.05$; Supplementary Figure S2 online), confirming the deleterious effect of p.Ala413Pro mutation in K14 on keratin filament network. In contrast, no keratin clumping was observed in normal human epidermal keratinocytes (NHEKs) transfected with any of the three plasmids (K14WT, K14A413T, and K14A413P; Supplementary Figure S3 online).

DISCUSSION

A single-nucleotide change in the protein-coding region that leads to an amino-acid substitution can be assigned either as a non-synonymous-coding single-nucleotide polymorphism or as a missense mutation. Numerous single-gene diseases have been attributed to missense mutations. However, it is sometimes difficult to demonstrate the effects of an amino-acid substitution on protein function and disease phenotype (Thusberg and Vihinen, 2009); it has been recently shown that the p.Met119Thr and p.Met119Val mutations in K14 result in EBS-DM and EBS-gen-non-DM, respectively (Cummins *et al.*, 2001). Our study provides a good model to study the pathogenicity of a single amino-acid substitution, as replacement of Ala^{413} in K14 with proline results in an EBS family, whereas replacement with threonine results in normal controls.

Ala^{413} is located in the helix termination motif of K14 and corresponds to position "*b*" of the heptad repeat (*abcdefg*) that is conserved among keratin polypeptides (Figure 3e), where "*a*" and "*d*" are usually non-polar amino acids and the others are polar or charged. Ala^{413} is highly conserved among species (Figure 3f).

Proline lacks an amide hydrogen atom and is unable to form a hydrogen bond with the carbonyl oxygen atom of the four amide residues N-terminal of it in an α-helix; thus, proline residues act as α-helix disruptors (although the stability of α-helices harboring a proline may be environment specific (Li *et al.*, 1996)). Previous reports using crystal X-ray analysis showed marked structural perturbations by proline residues in polypeptides (MacArthur and Thornton, 1991). Keratin has a conserved structure with helix motifs, and proline substitutions in these motifs have been reported to cause marked structural perturbations (Letai *et al.*, 1992). As for EBS, proline substitutions in K5/K14 have been described in 34 cases in the Human Intermediate Filament Database (http://www.interfil.org/; Szeverenyi *et al.*, 2008), although no non-synonymous-coding single-nucleotide polymorphisms have been detected in the database that cause proline substitutions. Clinical manifestations in EBS with proline substitutions vary between the localized and Dowling–Meara types, although proline substitutions in helix motifs tend to lead to EBS-DM, and those substitutions in domains outside helix motifs are more often observed in EBS-gen-non-DM.

A Taiwanese patient with EBS-loc has been described as heterozygous for p.Ala413Thr in K14 (Chao *et al.*, 2002). However, p.Ala413Thr was recently found in 6 of 112 alleles in normal Japanese individuals (Hattori *et al.*, 2006). Our study confirmed the presence of normal control individuals who are heterozygous for p.Ala413Thr (Figure 2b). Furthermore, a single normal control was homozygous for p.Ala413Thr (Figure 2c), which lowers the possibility of pathogenic effects from threonine substitution at this amino acid. Threonine and alanine substitute for one another on a frequency commensurate with their occurrence in structured proteins (Henikoff and Henikoff, 1992). Thus, structurally they can be considered interchangeable. Proline, on the other hand, is seldom observed to substitute for any residue, including alanine, highlighting its unique structural characteristics. Our *in vitro* study using HaCaT cells confirmed that it is not threonine substitution but proline substitution that causes keratin aggregation. Nevertheless, it is possible that p.Ala413Thr is a phenotypical mutation in

certain environmental conditions, as many contributing factors including temperature, trauma, and location of blister formation can affect the development of blistering phenotypes (Coulombe *et al.*, 2009).

Modeling of K5/K14 mutations in coiled-coil structures provides evidence that a correlation exists between the clinical severity of EBS and the degree of structural distortion caused by the underlying amino-acid change (Smith *et al.*, 2004). Our study has also demonstrated that MD simulations of keratin mutations accurately correlate with the pathogenicity of an amino-acid substitution.

As HaCaT cells are not normal keratinocytes, their keratin expression level is different from that of NHEK (Boukamp *et al.*, 1988). No keratin clumping was seen in NHEK transfected with any of K14WT, K14A413T, or K14A413P (Supplementary Figure S3 online). This result indicates that either overexpressed recombinant K14 is not enough to disrupt keratin network in NHEK due to a much higher expression of endogenous K14 in NHEK than in HaCaT cells (Sorensen *et al.*, 2003). On the other hand, the balance of keratin network may be substantially altered when recombinant K14 is overexpressed in HaCaT cells, in which endogenous K14 is reduced compared with NHEK (Sorensen *et al.*, 2003). The absence of keratin aggregation in the proband's skin keratinocytes (Figure 1c), compared with what was observed in HaCaT cells transfected with K14A413P, may reflect the greater effect of K14 mutant introduction in HaCaT cells compared with NHEK.

In summary, this study gives insight into consequences of two different amino-acid substitutions at the same codon. The biological effects of one amino-acid substitution are hard to predict. *In silico* and *in vitro* analyses are useful for confirming the pathogenicity of missense mutations.

MATERIALS AND METHODS

Mutation analysis

Genomic DNA extracted from peripheral blood was used as a template for PCR amplification. The *KRT5* and *KRT14* genes were amplified by methods previously described (Stephens *et al.*, 1997; Hut *et al.*, 2000). DNA sequencing of the PCR products was carried out with an ABI 3100 sequencer (PerkinElmer Life Sciences-ABI, Foster City, CA). The mutation nomenclature follows published mutation nomenclature guidelines (http://www.hgvs.org/mutnomen) according to the reference sequence NM_000424.3 for *KRT5* and NM_000526.3 for *KRT14*, with +1 as the A of the ATG initiation codon.

Mutant allele-specific amplification analysis

To verify the mutation, mutant allele-specific amplification analysis was performed with mutant allele-specific primers carrying the substitution of two bases at the 3′-end mutant allele-specific primers (Linard *et al.*, 2002; Sapio *et al.*, 2006): forward, 5′-ACGCG GCTGGAGCAGGAGATTC-3′ and reverse, 5′-GACAGCACTAGAGC TCAGCC-3′. PCR conditions were as follows: 94°C for 5 minutes, followed by 30 cycles of 94°C for 30 seconds, 65°C for 30 seconds, 72°C for 30 seconds, and extension at 72°C for 7 minutes.

Plasmid construction

cDNA containing the entire coding region of *KRT14* (K14WT) subcloned into the pcDNA 3.1/V5-His vector (Invitrogen, Carlsbad, CA) was employed (Yoneda *et al.*, 2004). The point-mutated *KRT14* cDNAs corresponding to the p.Ala413Pro (K14A413P) and p.Ala1237Thr (K14A413T) mutations were generated with the use of the GeneTailor Site-Directed Mutagenesis System (Invitrogen). Sense primers used for the PCR reactions to generate the K14A413P and the K14A413T fragments were 5′-CGCGGCTGGAGCAGGAGA TC**c**CCACCTACCGC-3′ and 5′-CGCGGCTGGAGCAGGAGATC**a**CCA CCTACCGC-3′, respectively (lower-case letters in bold denote mutations introduced). The anti-sense primer 5′-GATCTCCTGCTCCA GCCGCGTCTTCACGTC-3′ was used to generate both of the mutant *KRT14* cDNAs.

Molecular modeling

The structure of segment 2B in human vimentin (PDB 1GK6) (Herrmann *et al.*, 2000; Strelkov *et al.*, 2002, 2004) was used as a template in comparative modeling of the K5/K14 heterodimer and the two mutations (K14-A413P and K14-A413T: 2B-108,*b*) using the Modeller (9v7) program (Fiser and Sali, 2003). The nomenclature K14-A413P: 2B-108,*b* specifies residue 413 in chain K14, its position 108 within segment 2B, and its position *b* within the heptad repeat. From 25 models of each heterodimer, the structure with the lowest Modeller Objective function was subjected to MD simulation.

MD simulations using the GROMACS (v4.0) package of programs (Hess *et al.*, 2008) were performed using the OPLS-aa force field (Jorgensen and Tirado-Rives, 1988). Ionizable residues were assumed to be in their charged state, whereas the amine and carboxyl termini were assumed to be in their neutral form. Each molecule was solvated in a $75 \times 75 \times 75$ Å^3 water box; sodium and chloride ions were added to neutralize the system and provide a final ionic strength of 0.154 M. Protein and water (with ions) were coupled separately to a thermal bath at 300 K using velocity rescaling (Bussi *et al.*, 2007) applied with a coupling time of 0.1 ps, whereas the pressure was coupled to an isotropic barostat using a time constant of 1 ps and compressibility of 4.5×10^{-5} bar^{-1}. All simulations were performed with a single non-bonded cutoff of 10 Å and applying a neighbour-list update frequency of 10 steps (20 fs). The particle-mesh Ewald method was used to account for long-range electrostatics (Essman *et al.*, 1995), applying a grid width of 1.2 Å, and a fourth-order spline interpolation. Bond lengths were constrained using the LINCS algorithm (Hess, 2008; Hess *et al.*, 2008). All simulations consisted of an initial minimization of water molecules, followed by 100 ps of MD with the protein restrained. Following positional restraints of MD, all restraints on the protein were removed and MD continued for a further 50 ns. Coordinates were archived throughout the simulation at 100-ps intervals.

Cell culture and plasmid transfection

HaCaT-immortalized keratinocytes and HeLa cells were maintained in DMEM (GIBCO, Grand Island, NY) supplemented with 10% (v/v) fetal bovine serum. NHEKs from neonatal foreskin (Lonza, Allendale, NJ) were cultured in keratinocyte growth medium (Lonza). Three different transfections (K14WT, K14A413P, and K14A413T) into HaCaT cells or HeLa cells (2 μg of plasmid in six-well dishes) were performed using Lipofectamine LTX (Invitrogen) according

to the manufacturer's instructions. Three different plasmids (K14WT, K14A413P, and K14A413T) were transfected, respectively, into NHEK (5 μg of plasmid in six-well dishes) with electroporation using Amaxa Nucleofector apparatus (Amaxa, Cologne, Germany). Also, three different transfections into HaCaT cells, including K14A413P alone (2 μg of plasmid in six-well dishes), a combination of equal amounts of K14A413P (1 μg) and K14WT (1 μg; K14A413P/K14WT), and a combination of equal amounts of K14A413P (1 μg) and K14A413T (1 μg; K14A413P/K14A413T) were performed using Lipofectamine LTX (Invitrogen).

Immunoblot analysis

At 24 hours after transfection, HaCaT cells were lysed in Laemmli buffer (consisting of 62.5 mM Tris-HCl (pH 6.8), 3% SDS, and 5% mercaptoethanol) on ice for 10 minutes, cell debris was removed by centrifugation at 14,000 rpm for 5 minutes, and supernatant was collected. Supernatants were electrophoresed on a NuPAGE 4–12% bis-Tris gel (Invitrogen) and transferred to a polyvinylidene difluoride membrane. The membrane was incubated with horseradish peroxidase-conjugated anti-V5 antibody (Invitrogen) for 1 hour at room temperature, and the blots were detected using the ECL Plus Detection Kit (GE Healthcare, Waukesha, WI).

Confocal laser analysis

At 24 hours after transfection, the cells were washed with phosphate-buffered saline and fixed with methanol. A FITC-conjugated anti-V5 antibody (Invitrogen) was used to detect transfected cells. All cells were observed using a confocal laser-scanning microscope (Olympus Fluoview FV300, Tokyo, Japan). The cells with keratin aggregates were counted in five different areas, two from each experimental replicate (a mean of 42 cells from each replicate), as described previously (Yasukawa *et al.*, 2002), and the results obtained from the 10 counts were expressed as the mean ± SEM.

Ethics

The medical ethics committee of Hokkaido University Graduate School of Medicine approved all studies. The study was conducted according to the Declaration of Helsinki Principles. Participants or their legal guardians gave written informed consent.

CONFLICT OF INTEREST

The authors state no conflict of interest.

ACKNOWLEDGMENTS

We thank Ms Yuko Hayakawa for her technical assistance. This work was supported by Health and Labor Sciences research grants from the Ministry of Health, Labor, and Welfare of Japan (to HS) for Research on Measures for Intractable Diseases. BJS gratefully acknowledges infrastructure support from NHMRC IRIISS grant no. 361646 and a Victorian State Government OIS grant.

SUPPLEMENTARY MATERIAL

Supplementary material is linked to the online version of the paper at http://www.nature.com/jid

REFERENCES

Albers K, Fuchs E (1987) The expression of mutant epidermal keratin cDNAs transfected in simple epithelial and squamous cell carcinoma lines. *J Cell Biol* 105:791–806

Boukamp P, Petrussevska RT, Breitkreutz D, Hornung J, Markham A, Fusenig NE (1988) Normal keratinization in a spontaneously immortalized aneuploid human keratinocyte cell line. *J Cell Biol* 106:761–71

Bussi G, Donadio D, Parrinello M (2007) Canonical sampling through velocity rescaling. *J Chem Phys* 126:014101

Chao SC, Yang MH, Lee SF (2002) Novel KRT14 mutation in a Taiwanese patient with epidermolysis bullosa simplex (Kobner type). *J Formos Med Assoc* 101:287–90

Conway JF, Parry DAD (1990) Structural features in the heptad substructure and longer range repeats of two-stranded alpha-fibrous proteins. *Int J Biol Macromol* 12:328–34

Coulombe PA, Fuchs E (1990) Elucidating the early stages of keratin filament assembly. *J Cell Biol* 111:153–69

Coulombe PA, Hutton ME, Letai A, Hebert A, Paller AS, Fuchs E (1991) Point mutations in human keratin 14 genes of epidermolysis bullosa simplex patients: genetic and functional analyses. *Cell* 66:1301–11

Coulombe PA, Kerns ML, Fuchs E (2009) Epidermolysis bullosa simplex: a paradigm for disorders of tissue fragility. *J Clin Invest* 119:1784–93

Cummins RE, Klingberg S, Wesley J, Rogers M, Zhao Y, Murrell DF (2001) Keratin 14 point mutations at codon 119 of helix 1A resulting in different epidermolysis bullosa simplex phenotypes. *J Invest Dermatol* 117:1103–7

Essman U, Perela L, Berkowitz ML, Darden T, Lee H, Pedersen LG (1995) A smooth particle mesh Ewald method. *J Chem Phys* 103:8577–92

Fine JD, Eady RA, Bauer EA, Bauer JW, Bruckner-Tuderman L, Heagerty A *et al.* (2008) The classification of inherited epidermolysis bullosa (EB): Report of the Third International Consensus Meeting on Diagnosis and Classification of EB. *J Am Acad Dermatol* 58:931–50

Fiser A, Sali A (2003) Modeller: generation and refinement of homology-based protein structure models. *Methods Enzymol* 374:461–91

Groves RW, Liu L, Dopping-Hepenstal PJ, Markus HS, Lovell PA, Ozoemena L *et al.* (2010) A homozygous nonsense mutation within the *dystonin* gene coding for the coiled-coil domain of the epithelial isoform of BPAG1 underlies a new subtype of autosomal recessive epidermolysis bullosa simplex. *J Invest Dermatol* 130:1551–7

Hattori N, Komine M, Kaneko T, Shimazu K, Tsunemi Y, Koizumi M *et al.* (2006) A case of epidermolysis bullosa simplex with a newly found missense mutation and polymorphism in the highly conserved helix termination motif among type I keratins, which was previously reported as a pathogenic missense mutation. *Br J Dermatol* 155:1062–3

Hatzfeld M, Franke WW (1985) Pair formation and promiscuity of cytokeratins: formation *in vitro* of heterotypic complexes and intermediate-sized filaments by homologous and heterologous recombinations of purified polypeptides. *J Cell Biol* 101:1826–41

Hatzfeld M, Weber K (1990) The coiled coil of *in vitro* assembled keratin filaments is a heterodimer of type I and II keratins: use of site-specific mutagenesis and recombinant protein expression. *J Cell Biol* 110:1199–210

Henikoff S, Henikoff JG (1992) Amino acid substitution matrices from protein blocks. *Proc Natl Acad Sci USA* 89:10915–9

Herrmann H, Strelkov SV, Feja B, Rogers KR, Brettel M, Lustig A *et al.* (2000) The intermediate filament protein consensus motif of helix 2B: its atomic structure and contribution to assembly. *J Mol Biol* 298:817–32

Hess B (2008) P-LINCS: a parallel linear constraint solver for molecular simulation. *J Chem Theory Comput* 4:116–22

Hess B, Kutzner C, van der Spoel D, Lindahl E (2008) GROMACS 4: algorithms for highly efficient, load-balanced, and scalable molecular simulation. *J Chem Theory Comput* 4:435–47

Hut PH, v d Vlies P, Jonkman MF, Verlind E, Shimizu H, Buys CH *et al.* (2000) Exempting homologous pseudogene sequences from polymerase chain reaction amplification allows genomic keratin 14 hotspot mutation analysis. *J Invest Dermatol* 114:616–9

Jorgensen WL, Tirado-Rives J (1988) The OPLS potential functions for proteins. Energy minimizations for crystals of cyclic peptides of crambin. *J Am Chem Soc* 110:1657–66

Lane EB, Rugg EL, Navsaria H, Leigh IM, Heagerty AH, Ishida-Yamamoto A *et al.* (1992) A mutation in the conserved helix termination peptide of keratin 5 in hereditary skin blistering. *Nature* 356:244–6

Letai A, Coulombe PA, Fuchs E (1992) Do the ends justify the mean? Proline mutations at the ends of the keratin coiled-coil rod segment are more disruptive than internal mutations. *J Cell Biol* 116:1181–95

Li SC, Goto NK, Williams KA, Deber CM (1996) Alpha-helical, but not beta-sheet, propensity of proline is determined by peptide environment. *Proc Natl Acad Sci USA* 93:6676–81

Linard B, Bezieau S, Benlalam H, Labarriere N, Guilloux Y, Diez E *et al.* (2002) A ras-mutated peptide targeted by CTL infiltrating a human melanoma lesion. *J Immunol* 168:4802–8

MacArthur MW, Thornton JM (1991) Influence of proline residues on protein conformation. *J Mol Biol* 218:397–412

Moll R, Franke WW, Schiller DL, Geiger B, Krepler R (1982) The catalog of human cytokeratins: patterns of expression in normal epithelia, tumors and cultured cells. *Cell* 31:11–24

Nelson WG, Sun TT (1983) The 50- and 58-kdalton keratin classes as molecular markers for stratified squamous epithelia: cell culture studies. *J Cell Biol* 97:244–51

Sapio MR, Posca D, Troncone G, Pettinato G, Palombini L, Rossi G *et al.* (2006) Detection of BRAF mutation in thyroid papillary carcinomas by mutant allele-specific PCR amplification (MASA). *Eur J Endocrinol* 154:341–8

Schweizer J, Bowden PE, Coulombe PA, Langbein L, Lane EB, Magin TM *et al.* (2006) New consensus nomenclature for mammalian keratins. *J Cell Biol* 174:169–74

Smith TA, Steinert PM, Parry DAD (2004) Modeling effects of mutations in coiled-coil structures: case study using epidermolysis bullosa simplex mutations in segment 1a of K5/K14 intermediate filaments. *Proteins* 55:1043–52

Sorensen CB, Andresen BS, Jensen UB, Jensen TG, Jensen PK, Gregersen N *et al.* (2003) Functional testing of keratin 14 mutant proteins associated with the three major subtypes of epidermolysis bullosa simplex. *Exp Dermatol* 12:472–9

Steinert PM (1990) The two-chain coiled-coil molecule of native epidermal keratin intermediate filaments is a type I-type II heterodimer. *J Biol Chem* 265:8766–74

Steinert PM, Marekov LN, Parry DAD (1993) Conservation of the structure of keratin intermediate filaments: molecular mechanism by which different keratin molecules integrate into preexisting keratin intermediate filaments during differentiation. *Biochemistry* 32:10046–56

Stephens K, Ehrlich P, Weaver M, Le R, Spencer A, Sybert VP (1997) Primers for exon-specific amplification of the *KRT5* gene: identification of novel and recurrent mutations in epidermolysis bullosa simplex patients. *J Invest Dermatol* 108:349–53

Strelkov SV, Herrmann H, Geisler N, Wedig T, Zimbelmann R, Aebi U *et al.* (2002) Conserved segments 1A and 2B of the intermediate filament dimer: their atomic structures and role in filament assembly. *EMBO J* 21:1255–66

Strelkov SV, Schumacher J, Burkhard P, Aebi U, Herrmann H (2004) Crystal structure of the human lamin A coil 2B dimer: implications for the head-to-tail association of nuclear lamins. *J Mol Biol* 343: 1067–80

Szeverenyi I, Cassidy AJ, Chung CW, Lee BT, Common JE, Ogg SC *et al.* (2008) The Human Intermediate Filament Database: comprehensive information on a gene family involved in many human diseases. *Hum Mutat* 29:351–60

Thusberg J, Vihinen M (2009) Pathogenic or not? And if so, then how? Studying the effects of missense mutations using bioinformatics methods. *Hum Mutat* 30:703–14

Yasukawa K, Sawamura D, Goto M, Nakamura H, Jung SY, Kim SC *et al.* (2006) Epidermolysis bullosa simplex in Japanese and Korean patients: genetic studies in 19 cases. *Br J Dermatol* 155:313–7

Yasukawa K, Sawamura D, McMillan JR, Nakamura H, Shimizu H (2002) Dominant and recessive compound heterozygous mutations in epidermolysis bullosa simplex demonstrate the role of the stutter region in keratin intermediate filament assembly. *J Biol Chem* 277: 23670–4

Yoneda K, Furukawa T, Zheng YJ, Momoi T, Izawa I, Inagaki M *et al.* (2004) An autocrine/paracrine loop linking keratin 14 aggregates to tumor necrosis factor alpha-mediated cytotoxicity in a keratinocyte model of epidermolysis bullosa simplex. *J Biol Chem* 279: 7296–303

xeroderma pigmentosum skin *in vitro*: a model to study hypersensitivity to UV light. *Photochem Photobiol* 81:19–24

Epp N, Fürstenberger G, Müller K *et al.* (2007) 12R-lipoxygenase deficiency disrupts epidermal barrier function. *J Cell Biol* 177:173–82

Gache Y, Baldeschi C, Del RM *et al.* (2004) Construction of skin equivalents for gene therapy of recessive dystrophic epidermolysis bullosa. *Hum Gene Ther* 15:921–33

García M, Larcher F, Hickerson RP *et al.* (2011) Development of skin-humanized mouse models of pachyonychia congenita. *J Invest Dermatol* 131:1053–60

Green H (1978) Cyclic AMP in relation to proliferation of the epidermal cell: a new view. *Cell* 15:801–11

Lampert IA (1985) Expression of class II MHC antigen on epithelia and autoimmunity. *Lancet* 2:1078

Leigh I, Watt F (1994) *Keratinocyte Methods.* Cambridge: Cambridge University Press

Mildner M, Ballaun C, Stichenwirth M *et al.* (2006) Gene silencing in a human organotypic skin model. *Biochem Biophys Res Commun* 348:76–82

Mildner M, Jin J, Eckhart L *et al.* (2010) Knockdown of filaggrin impairs diffusion barrier function and increases UV sensitivity in a human skin model. *J Invest Dermatol* 130:2286–94

O'Shaughnessy RF, Choudhary I, Harper JI (2010) Interleukin-1 alpha blockade prevents hyperkeratosis in an *in vitro* model of lamellar ichthyosis. *Hum Mol Genet* 19:2594–605

Oji V, Eckl KM, Aufenvenne K *et al.* (2010) Loss of corneodesmosin leads to severe skin barrier defect, pruritus, and atopy: unraveling the peeling skin disease. *Am J Hum Genet* 87:274–81

Rheinwald JG, Green H (1975) Serial cultivation of strains of human epidermal keratinocytes: the formation of keratinizing colonies from single cells. *Cell* 6:331–43

Schäfer-Korting M, Bock U, Diembeck W *et al.* (2008) The use of reconstructed human epidermis for skin absorption testing: results of the validation study. *Altern Lab Anim* 36:161–87

Thomas AC, Tattersall D, Norgett EE *et al.* (2009) Premature terminal differentiation and a reduction in specific proteases associated with loss of ABCA12 in Harlequin ichthyosis. *Am J Pathol* 174:970–8

Tjabringa G, Bergers M, van Rens D *et al.* (2008) Development and validation of human psoriatic skin equivalents. *Am J Pathol* 173: 815–23

Williams ML (1992) Ichthyosis: mechanisms of disease. *Pediatr Dermatol* 9:365–8

AKT Has an Anti-Apoptotic Role in ABCA12-Deficient Keratinocytes

Journal of Investigative Dermatology (2011) **131,** 1942–1945; doi:10.1038/jid.2011.132; published online 2 June 2011

TO THE EDITOR

Harlequin ichthyosis (HI) is a hereditary skin disorder characterized by severe hyperkeratosis and impaired skin barrier function (Moskowitz *et al.*, 2004; Akiyama *et al.*, 2005). We have identified the ATP-binding cassette transporter A12 (*ABCA12*) as the causative gene of HI and, furthermore, demonstrated that ABCA12 is essential for keratinocyte lipid transport (Akiyama *et al.*, 2005; Yanagi *et al.*, 2008). Loss of ABCA12 function causes lipid transport to be defective in keratinocytes of the upper spinous and granular layers, resulting in the deposition of numerous intracellular lipid droplets and malformation of intercellular lipid layers (Akiyama *et al.*, 2005; Yanagi *et al.*, 2010). Recently, we have shown that gangliosides accumulate in the differentiated keratinocytes of HI patients (Mitsutake *et al.*, 2010). On the basis of the evidence that lipid accumulation is involved in keratinocyte apoptosis (Wang *et al.*, 2001; Uchida *et al.*, 2010), we investigated apoptotic and anti-apoptotic parameters in skin samples from HI patients and *Abca12*$^{-/-}$ HI model mice.

We studied the skin of two HI patients and that of *Abca12*$^{-/-}$ mice. The *ABCA12* mutations of the two HI patients have been previously reported: one patient has the homozygous splice acceptor site mutation c.3295-2A>G and the other has the homozygous nonsense mutation p.Arg434X (Akiyama *et al.*, 2005). The procedure for generating *Abca12*$^{-/-}$ mice, the establishment of primary-cultured keratinocytes, immunofluorescence staining, immunoblotting, and real-time reverse transcriptase PCR analysis has been previously described (Yanagi *et al.*, 2008, 2010). First, we investigated the apoptosis of HI patient epidermis by hematoxylin–eosin stain and TUNEL assay (*In situ* Apoptosis Detection Kit, Takara Bio, Otsu, Japan). In the HI patients, the nuclei of the granular-layer keratinocytes were condensed (Figure 1b) and they show positive for TUNEL labeling (Figure 1d), although apoptotic nuclei are rare in the normal human epidermis (Figure 1a, c). The histopathological findings and results of TUNEL staining of the *Abca12*$^{-/-}$ mice were similar to those in the skin of the HI patients (Figure 1f and h). TUNEL staining in the epidermis of 18.5-day embryos indicated that the apoptosis of keratinocytes started during fetal skin development (Figure 1j).

We assessed the degree of AKT activation of *Abca12*$^{-/-}$ skin and keratinocytes using anti-AKT antibody #4691 and anti-phosphorylated AKT (Ser473) #4060 antibody (Cell Signaling, Danvers, MA). By immunoblot analysis, differentiated primary-cultured keratinocytes and the epidermis of *Abca12*$^{-/-}$ mice showed higher expression levels of Ser-473 phosphorylated AKT than those of the control wild-type mice (Figure 1o). Immunofluorescence staining detected phosphorylated AKT in the upper granular-layer keratinocytes of the *Abca12*$^{-/-}$ mouse skin (Figure 1l), but not in the skin of control wild-type mouse (Figure 1k). Cell proliferation was assessed by Ki-67 immunofluorescence (Figure 1). Ki-67 stain was similar in the wild-type and the *Abca12*$^{-/-}$ samples, indicating that the granular-layer keratinocytes of the *Abca12*$^{-/-}$ neonatal mice showed no excessive cell proliferation. To clarify whether AKT activation has

Abbreviations: ABCA12, ATP-binding cassette transporter A12; HI, harlequin ichthyosis; PPAR, peroxisome proliferator-activated receptor; RXR, retinoid X receptor

anti-apoptotic effects on *Abca12*$^{-/-}$ keratinocytes, we performed TUNEL staining of keratinocytes treated with AKT inhibitor, which blocks AKT phosphorylation (#124017; InSolution Akt Inhibitor VIII, Calbiochem, San Diego, CA). *Abca12*$^{-/-}$ keratinocytes incubated with 10 μM #124017 AKT inhibitor showed a notably greater number of TUNEL-positive cells than both wild-type keratinocytes with AKT inhibitor and *Abca12*$^{-/-}$ keratinocytes without AKT inhibitor (Figure 2). These results suggest that AKT activation helps *Abca12*$^{-/-}$ keratinocytes to avoid apoptosis. Furthermore, mRNA and protein levels of peroxisome proliferator-activated receptor (PPAR)-δ from *Abca12*$^{-/-}$ epidermis were shown to be significantly higher than those from wild-type epidermis (Taqman Gene Expression Assay, probe ID, Mm00803184_m1, Mm99999915_g1, Applied Biosystems, Carlsbad, CA; anti-PPAR-δ antibody H-74, Santa Cruz, Santa Cruz, CA; Supplementary Figure S1 online), which suggests upregulation of PPAR-δ as a candidate pathway for AKT activation.

Herein, we have suggested that apoptosis is involved in the pathomechanism of HI. Defective lipid transport due to loss of ABCA12 function leads to the accumulation of intracellular lipids, including glucosylceramides and gangliosides (Akiyama *et al.*, 2005; Mitsutake *et al.*, 2010). Studies by Wang *et al.* (2001) and Sun *et al.* (2002) showed that the elevation of ganglioside levels leads to keratinocyte apoptosis. Thus, we are able to speculate that the accumulation of gangliosides leads to the apoptosis of *Abca12*$^{-/-}$ keratinocytes, although the exact mechanism of apoptosis in *Abca12*$^{-/-}$ keratinocytes remains unclear.

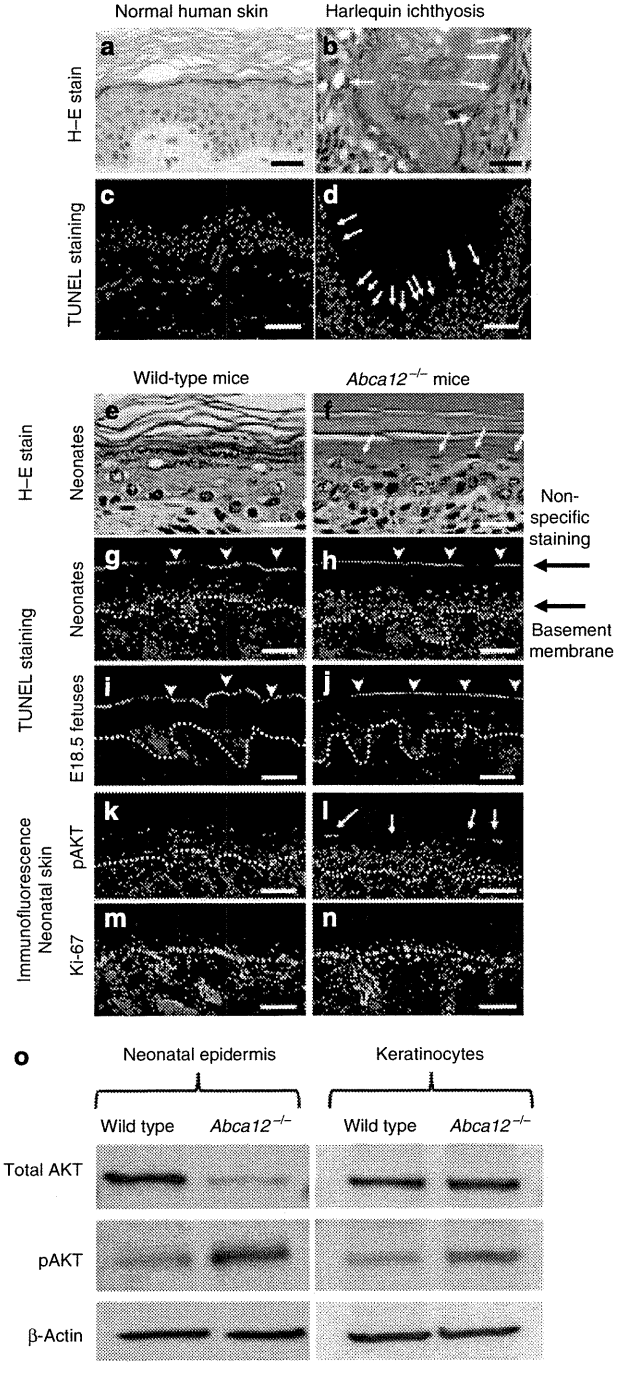

Figure 1. ATP-binding cassette transporter A12-deficient keratinocytes show TUNEL-positive nuclei and AKT activation. (**a**–**d**) In the harlequin ichthyosis patients, the nuclei of the granular-layer keratinocytes are condensed (**b**, white arrows) and they show positive TUNEL labeling (**d**, white arrows), although apoptotic nuclei are rare in the normal human epidermis (**a**, **c**). Data shown are representative of those from the two harlequin ichthyosis patients. (**e**, **f**) Granular-layer keratinocytes of *Abca12*$^{-/-}$ mice show more condensed nuclei (**f**, white arrows) than those of wild-type mice (**e**). (**g**–**j**) Granular-layer keratinocytes of *Abca12*$^{-/-}$ mice, a neonate (**h**) and an 18.5-day embryo (**j**), show TUNEL-positive nuclei. No TUNEL-positive cells are seen in the epidermis of the control wild-type mice (**g**, **i**). Dotted lines indicate the basement membrane. Nonspecific staining is seen on the skin surface (white arrowheads). (**k**, **l**) By immunofluorescence staining, AKT activation (Ser-473 phosphorylated AKT; green) is observed in granular-layer keratinocytes of *Abca12*$^{-/-}$ mice. (**m**, **n**) Immunofluorescence staining for the Ki-67-proliferation marker shows similar staining patterns of basal keratinocytes in wild-type (**m**) and *Abca12*$^{-/-}$ (**n**) samples. (**a**, **b**, **e**, **f**; hematoxylin–eosin (H–E) stain. Bars of **c**, **d**, **g**, **h**, **i**, **j**, **k**, **l**, **m**, **n** = 20 μm. Bars of **a**, **b**, **e**, **f** = 5 μm.) (**o**) Immunoblot analysis shows that levels of serine-473-phosphorylated AKT (pAKT) in neonatal epidermis and differentiated keratinocytes of *Abca12*$^{-/-}$ mice are higher than those of wild-type mice.

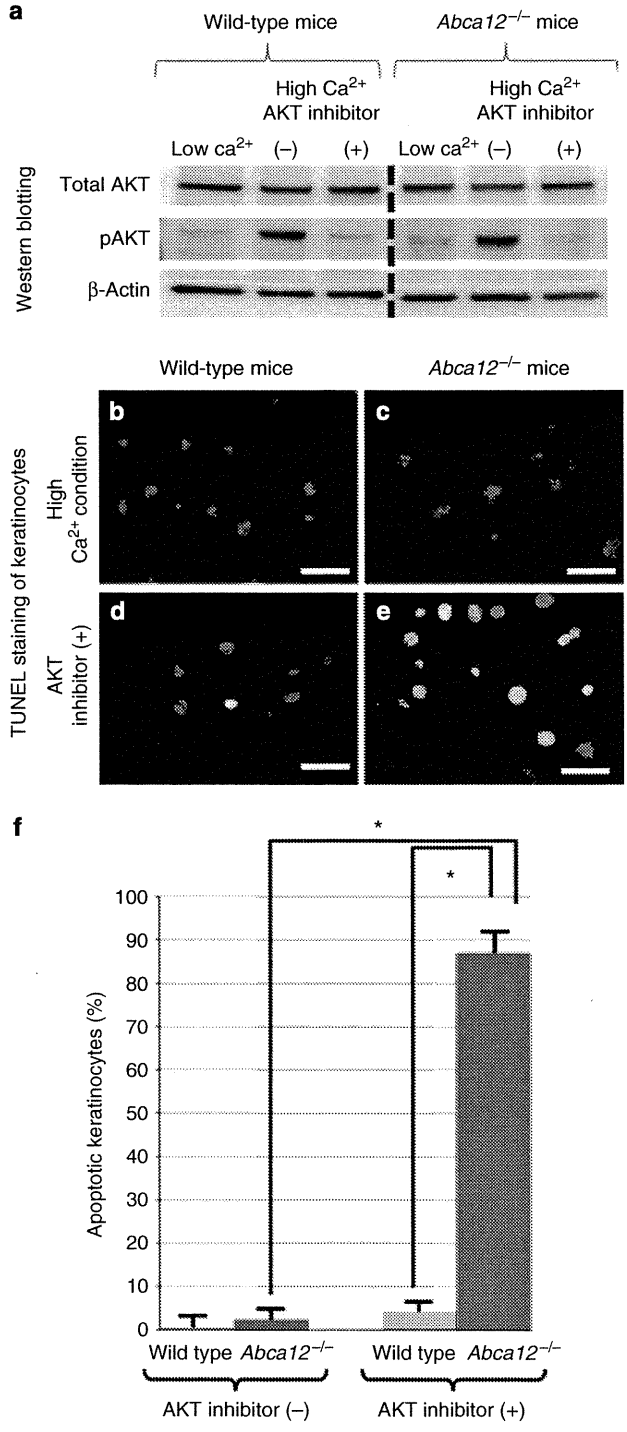

Figure 2. Inhibition of AKT activation leads to apoptosis of *Abca12*$^{-/-}$ keratinocytes. (**a**) Immunoblot analysis indicates that the AKT inhibitor can inhibit AKT activation (phosphorylated AKT (pAKT) synthesis) in differentiated keratinocytes. (**b–e**) TUNEL staining of keratinocytes cultured under high Ca^{2+} condition treated with/without the AKT inhibitor. Neither wild-type cells (**b**) nor *Abca12*$^{-/-}$ cells (**c**) are TUNEL positive. *Abca12*$^{-/-}$ keratinocytes with the AKT inhibitor (#124017; 10 μM) show many TUNEL-positive nuclei (**e**), although only a small number of wild-type cells with the AKT inhibitor are TUNEL positive (**d**). (Bars = 20 μm.) (**f**) Percentage of TUNEL-positive keratinocytes. *Abca12*$^{-/-}$ keratinocytes with AKT inhibitor shows a significantly greater number of TUNEL-positive nuclei than wild-type keratinocytes with/without the AKT inhibitor and *Abca12*$^{-/-}$ keratinocytes without the AKT inhibitor. ($n = 3$, mean ± SD, $^*P < 0.05$).

Although *Abca12*$^{-/-}$ granular-layer keratinocytes show characteristics of apoptosis, including condensed nuclei and positive TUNEL labeling, they are able to form epidermal stratification. In several disorders involving keratinocyte apoptosis, e.g., toxic epidermal necrolysis, the apoptotic epidermal keratinocytes show not only TUNEL-positive nuclei but also defective epidermal stratification (Abe *et al.*, 2003). Thrash *et al.* (2006) reported that AKT1 activation is an essential signal for keratinocyte cell survival and stratification, by experiments with gene silencing and three-dimensional cell cultures. Thus, we hypothesized that the AKT pathway might work as a compensatory mechanism against apoptosis in *Abca12*$^{-/-}$ keratinocytes. We have clearly shown that AKT activation occurs in *Abca12*$^{-/-}$ granular-layer keratinocytes, which suggests that AKT activation serves to prevent the cell death of *Abca12*$^{-/-}$ keratinocytes. By immunoblot analysis using anti-AKT1/2/3 antibodies (#2938/3063/3788, Cell Signaling), *Abca12*$^{-/-}$ epidermis showed expression of AKT1 and AKT2, but not AKT3 (Supplementary Figure S2 online). Compared with wild-type epidermis, *Abca12*$^{-/-}$ epidermis seemed to have more AKT1 than AKT2. From our data and the literature (Thrash *et al.*, 2006), we are able to speculate that AKT1 is the major isoform of phosphorylated AKT in *Abca12*$^{-/-}$ epidermis.

We have shown that PPAR-δ is a candidate molecule in the upstream of the AKT activation pathway in *Abca12*$^{-/-}$ keratinocytes. Di-Poi *et al.* (2002) reported that PPAR-δ has an anti-apoptotic role in keratinocytes via transcriptional control of the AKT1 signaling pathway. PPAR-δ also regulates the expression of ABCA12 (Jiang *et al.*, 2008). From these studies, we can speculate that upregulation of PPAR-δ is in response to apoptosis or decreased ABCA12 expression. To ascertain the function of PPAR-δ, we performed the experiments using a PPAR-δ-specific antagonist (GSK0660, Santa Cruz). Differentiated *Abca12*$^{-/-}$ keratinocytes treated with 1 μM GSK0660 for 48 hours showed TUNEL-positive nuclei, from which we are able to speculate an anti-apoptotic role for

PPAR-δ in *Abca12*$^{-/-}$ keratinocytes (Supplementary Figure S1 online). From our studies and the literature (Di-Poi *et al.*, 2002), PPAR-δ has been shown to have at least an anti-apoptotic role in *Abca12*$^{-/-}$ keratinocytes; however, it remains unclear whether the upregulation of PPAR-δ is in response to apoptosis or decreased ABCA12 expression.

Furthermore, we have measured the mRNA expression levels of other nuclear hormone receptors, including PPAR-α, PPAR-γ, retinoic acid receptor-α, liver X receptor-α, liver X receptor-β, RXR-α, and RXR-γ (Applied Biosystems). The mRNA level of RXR-α from *Abca12*$^{-/-}$ epidermis was shown to be significantly higher than that from wild-type epidermis (Supplementary Figure S1 online). The interaction between the upregulation of RXR-α and AKT activation in keratinocytes has not been reported. However, Wang *et al.* (2011) reported that RXR-α ablation in the epidermis enhances UV-induced apoptosis, which suggests that RXR-α has an anti-apoptotic function in keratinocytes. Thus, upregulation of RXR-α may also have an anti-apoptotic function in *Abca12*$^{-/-}$ keratinocytes.

In conclusion, the present data suggest that keratinocyte apoptosis is involved in the pathomechanisms of HI and that the AKT signaling pathway helps *Abca12*$^{-/-}$ keratinocytes to survive during the keratinization process. In light of this, activation of the AKT signal pathway may be to our knowledge, previously unreported strategy for treating keratinization disorders, including ichthyosis.

CONFLICT OF INTEREST

The authors state no conflict of interest.

ACKNOWLEDGMENTS

We thank Ms Aoyanagi for her technical assistance. This work was supported in part by a grant-in-aid from the Ministry of Education, Science, Sports and Culture of Japan (Kiban A 23249058: to MA), a grant from the Ministry of Health, Labor and Welfare of Japan (Health and Labor Sciences Research Grants; Research on Intractable Disease: H22-177: to MA), and a grant-in-aid from the Japan Society for the Promotion of Science Fellows (to TY).

***Teruki Yanagi*[1], *Masashi Akiyama*[1,2], *Hiroshi Nishihara*[3], *Yuki Miyamura*[1], *Kaori Sakai*[1], *Shinya Tanaka*[4] *and Hiroshi Shimizu*[1]**

[1]Department of Dermatology, Hokkaido University Graduate School of Medicine, Sapporo, Japan; [2]Department of Dermatology, Nagoya University Graduate School of Medicine, Nagoya, Japan; [3]Laboratory of Translational Pathology, Hokkaido University Graduate School of Medicine, Sapporo, Japan and [4]Laboratory of Cancer Research, Department of Pathology, Hokkaido University Graduate School of Medicine, Sapporo, Japan
E-mail: makiyama@med.nagoya-u.ac.jp

SUPPLEMENTARY MATERIAL

Supplementary material is linked to the online version of the paper at http://www.nature.com/jid

REFERENCES

Abe R, Shimizu T, Shibaki A *et al.* (2003) Toxic epidermal necrolysis and Stevens-Johnson syndrome are induced by soluble Fas ligand. *Am J Pathol* 162:1515–20

Akiyama M, Sugiyama-Nakagiri Y, Sakai K *et al.* (2005) Mutations in lipid transporter ABCA12 in harlequin ichthyosis and functional recovery by corrective gene transfer. *J Clin Invest* 115:1777–84

Di-Poi N, Tan NS, Michalik L *et al.* (2002) Antiapoptotic role of PPARbeta in keratinocytes via transcriptional control of the Akt1 signaling pathway. *Mol Cell* 10:721–33

Jiang YJ, Lu B, Kim P *et al.* (2008) PPAR and LXR activators regulate ABCA12 expression in human keratinocytes. *J Invest Dermatol* 128:104–9

Mitsutake S, Suzuki C, Akiyama M *et al.* (2010) ABCA12 dysfunction causes a disorder in glucosylceramide accumulation during keratinocyte differentiation. *J Dermatol Sci* 60:128–9

Moskowitz DG, Fowler AJ, Heyman MB *et al.* (2004) Pathophysiologic basis for growth failure in children with ichthyosis: an evaluation of cutaneous ultrastructure, epidermal permeability barrier function, and energy expenditure. *J Pediatr* 145:82–92

Sun P, Wang XQ, Lopatka K *et al.* (2002) Ganglioside loss promotes survival primarily by activating integrin-linked kinase/Akt without phosphoinositide 3-OH kinase signaling. *J Invest Dermatol* 119:107–17

Thrash BR, Menges CW, Pierce RH *et al.* (2006) AKT1 provides an essential survival signal required for differentiation and stratification of primary human keratinocytes. *J Biol Chem* 281:12155–62

Uchida Y, Houben E, Park K *et al.* (2010) Hydrolytic pathway protects against ceramide-induced apoptosis in keratinocytes exposed to UVB. *J Invest Dermatol* 130: 2472–80

Wang XQ, Sun P, Paller AS (2001) Inhibition of integrin-linked kinase/protein kinase B/Akt signaling: mechanism for ganglioside-induced apoptosis. *J Biol Chem* 276:44504–11

Wang Z, Coleman DJ, Bajaj G *et al.* (2011) RXRalpha ablation in epidermal keratinocytes enhances UVR-induced DNA damage, apoptosis, and proliferation of keratinocytes and melanocytes. *J Invest Dermatol* 131:177–87

Yanagi T, Akiyama M, Nishihara H *et al.* (2008) Harlequin ichthyosis model mouse reveals alveolar collapse and severe fetal skin barrier defects. *Hum Mol Genet* 17:3075–83

Yanagi T, Akiyama M, Nishihara H *et al.* (2010) Self-improvement of keratinocyte differentiation defects during skin maturation in ABCA12-deficient harlequin ichthyosis model mice. *Am J Pathol* 177:106–18

See related commentary on pg 1790

Interpretation of Skindex-29 Scores: Cutoffs for Mild, Moderate, and Severe Impairment of Health-Related Quality of Life

Journal of Investigative Dermatology (2011) **131,** 1945–1947; doi:10.1038/jid.2011.138; published online 19 May 2011

TO THE EDITOR

Health-related quality of life (HRQL) is commonly assessed by means of standardized questionnaires and expressed in domain and overall HRQL scores. An important challenge is to interpret these scores correctly. What does a given score really mean? Although there is no standard approach, several methods exist to facilitate the interpretation of HRQL scores.

In a recently published study (Prinsen *et al.*, 2010), we identified

Abbreviation: HRQL, health-related quality of life

Recurrence of Hydroxyurea-induced Leg Ulcer After Discontinuation of Treatment

Kazuhiro Kikuchi[1], Ken Arita[1], Yasuki Tateishi[1], Masahiro Onozawa[2], Masashi Akiyama[1] and Hiroshi Shimizu[1]
Departments of [1]Dermatology and [2]Hematology, Hokkaido University Graduate School of Medicine, North 15 West 7, Kita-ku, Sapporo 060-8638, Japan.
E-mail: kikku@med.hokudai.ac.jp
Accepted November 1, 2010.

Hydroxyurea (HU) is a hydroxylated derivative of urea that has been recognized since 1960 as effective against cancer (1). It is an inhibitor of cellular DNA synthesis, and it promotes cell death in the S phase of the cell cycle through inhibition of the enzyme ribonucleotide reductase (2). The most common indications for HU therapy are chronic myeloid leukaemia and other myeloproliferative disorders (3, 4) such as essential thrombocythemia (5) and polycythemia vera (PV) (6). Cutaneous side-effects, such as alopecia, diffuse hyperpigmentation, scaling, lichen planus-like lesions, poikiloderma, atrophy of the skin and subcutaneous tissues, and nail changes, can occur during the treatment with HU (7–9). The occurrence of painful leg ulcers represents another rare and incompletely characterized complication that has been described in patients with myeloproliferative diseases receiving high-dose long-term HU treatment (10). While the mode of action of HU on bone marrow elements is well established, its effects on actively proliferating epithelial cells remain less described (11). Poor response to traditional local and systemic therapy is a typical feature of HU-induced leg ulcers, and discontinuation of the drug is often required to achieve complete wound healing (6, 8). Cessation of the drug usually improves the skin ulcer; although, in some cases, the ulcer remains and additional therapies, such as skin grafting, are needed (12). We report here the first case of a leg ulcer that recurred even after discontinuation of HU treatment.

CASE REPORT

The patient was an 82-year-old Japanese male who had been diagnosed with PV 9 years before and had been treated only with phlebotomy and an anti-platelet agent for several years. Due to splenomegaly and elevated blood cell counts, HU therapy was started 3 years ago at a dosage of 1 g daily for a month, followed by 1.0 or 1.5 g daily for 28 months. A good clinical response was achieved. However, the patient developed painful ulcers on the left second toe after two years of HU treatment.

He visited our outpatient clinic and was diagnosed with an HU-induced skin ulcer. HU was discontinued, topical application of sulfadiazine silver was performed, an oral antibiotic (cefdinir) was administered, and the ulcer epithelialized. However, a new ulcer appeared on the left lateral malleolar area 46 days after cessation of HU and gradually enlarged in size. The patient was admitted to our hospital for treatment of the ulcer.

Examination revealed a 48 × 56 mm ulcer with yellow necrotic tissue and marginal erythematous oedema (Fig. 1). Laboratory examination revealed a white blood cell count of $11.6 \times 10^3/\mu l$, a platelet count of $64.2 \times 10^4/l$, and a red blood cell count of $5.07 \times 10^6/\mu l$. Anti-nuclear antibody, anti-neutrophilic cytoplasmic antibodies, anti-cardiolipin antibody, and cryoglobulin were negative. A skin biopsy taken from the margin of the ulcer demonstrated leukocytoclastic vasculitis in the upper dermis (Fig. 2). A wound-healing strategy of surgical debridement, intravenous prostaglandin E1 administration, and topical application of beta-fibroblast growth factor, sulfadiazine silver and alprostadil alfadex was started, and the ulcer began to epithelialize. After 4 months, re-epithelialization was complete. The PV was treated with busulfan, achieving a good clinical response.

DISCUSSION

HU is usually well tolerated and has low toxicity (1). However, cutaneous adverse effects such as diffuse hyperpigmentation, brown discoloration of the nails, acral erythema, photosensitization, fixed drug eruption, alopecia, and oral ulceration have been reported (7–9). Stahl & Silber (10) first reported HU-induced skin ulcers in 1985. Montefusco et al. (11) reported

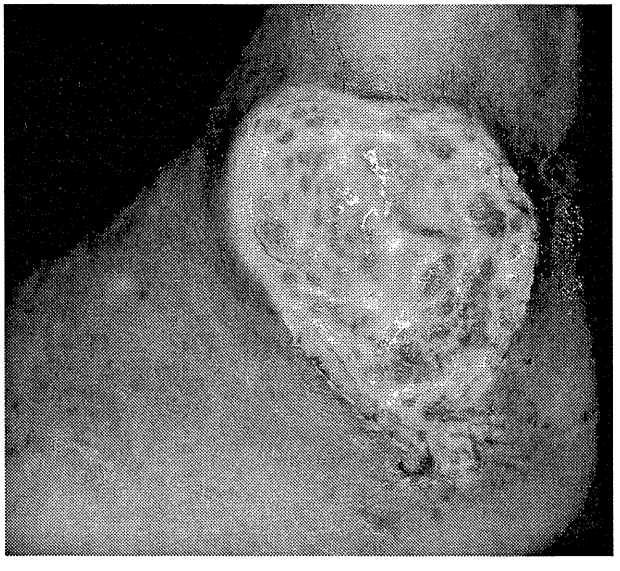

Fig. 1. Left foot with an ulcer on the lateral malleolar area after two months free of hydroxyurea administration. The ulcer was covered with yellow necrotic tissue and surrounded by oedematous erythema.

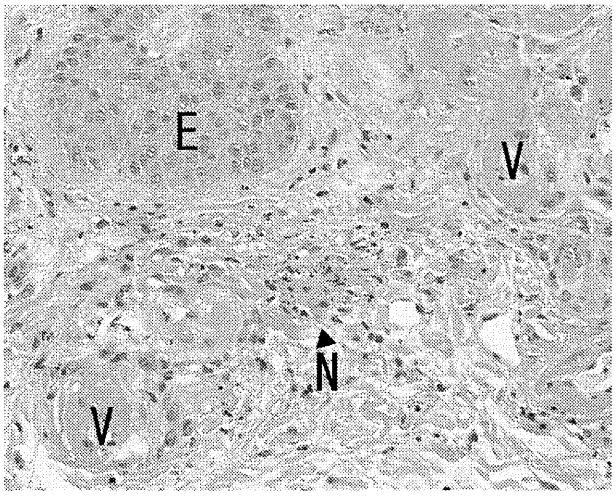

Fig. 2. Histology of erythema on the margin of the ulcer (haematoxylin-eosin staining). Fibrin deposition on the vascular wall and nucleic debris were evident around small vessels (×100). (E: epidermis; V: blood vessels; N: neutrophilic nuclear debris)

that, among 200 chronic myeloid leukaemia patients treated with HU, 17 (8.5%) developed leg ulcers. However, they achieved complete resolution or significant improvement after discontinuation of HU therapy (11). HU-induced leg ulcer and complete resolution within several months after drug discontinuation has also been reported in other myeloproliferative disorder, such as PV (6) and essential thrombocythemia (5). In those cases, as in ours, most of the patients had been treated with > 1 g of HU per day for at least one year (8). In the present case, the patient was treated with > 1 g of HU per day for 28 months. The ulcer occurred on his lateral malleolus, which histologically showed leukocytoclastic vasculitis. These features are consistent with previous reports of HU-induced leg ulcer.

From previous reports, the pathogenesis of HU-induced ulceration remains unclear and it may be multifactorial. It has been postulated that ulcers may be the result of: (*i*) interruption of microcirculation due to leukocytoclastic vasculitis or arterial microthrombi related to platelet dysregulation (13, 14); (*ii*) cumulative toxicity in the basal layer of the epidermis through inhibition of DNA synthesis (8); and (*iii*) repeated mechanical injury in areas subject to trauma: a perimalleolar area for instance (15).

In the case described here, a new ulcer developed even after cessation of HU administration. As for the pathogenic mechanism of recurrence, (*i*) interruption of microcirculation could result from hyperviscosity due to the elevated platelet count (as high as 100×10^4/l in one measurement) (13, 14), although no thrombi were observed histologically in the capillaries or small vessels. (*ii*) The direct cytotoxic effect of HU (8) may continue even after the withdrawal of the drug, and it may inhibit the repair of (*iii*) small injuries in the perimalleolar area: the one of the area susceptible to physical trauma (15). These assumptions can be made from the pathogenesis of HU-induced ulcer reported previously (8, 13–15).

To our knowledge, this is the first report of recurrence of HU-related leg ulcer after the discontinuation of medication. The case suggests that it is important to pay careful attention to recurrence even after cessation of HU therapy. Precise, early treatment for microtraumas and small ulcers should be administered to patients with a long history of HU medication.

REFERENCES

1. Boyd AS, Neldner KH. Hydroxyurea therapy. J Am Acad Dermatol 1991; 25: 518–524.
2. Yarbro JW. Mechanism of action of hydroxyurea. Semin Oncol 1992; 19: 1–10.
3. Goldman JM. Therapeutic strategies for chronic myeloid leukemia in the chronic (stable) phase. Semin Hematol 2003; 40: 10–17.
4. Rice L, Baker KR. Current management of the myeloproliferative disorders: a case-based review. Arch Pathol Lab Med 2006; 130: 1151–1156.
5. Demirçay Z, Cömert A, Adigüzel C. Leg ulcers and hydroxyurea: report of three cases with essential thrombocythemia. Int J Dermatol 2002; 41: 872–874.
6. Bader U, Banyai M, Böni R, Burg G, Hafner J. Leg ulcers in patients with myeloproliferative disorders: disease- or treatment-related? Dermatology 2000; 200: 45–48.
7. Najean Y, Rain JD. Treatment of polycythemia vera: the use of hydroxyurea and pipobroman in 292 patients under the age of 65 years. Blood 1997; 90: 3370–3377.
8. Weinlich G, Schuler G, Greil R, Kofler H, Fritsch P. Leg ulcers associated with long-term hydroxyurea therapy. J Am Acad Dermatol 1998; 39: 372–374.
9. Daoud MS, Gibson LE, Pittelkow MR. Hydroxyurea dermopathy: a unique lichenoid eruption complicating long-term therapy with hydroxyurea. J Am Acad Dermatol 1997; 36: 178–182.
10. Stahl RL, Silber R. Vasculitic leg ulcers in chronic myelogenous leukemia. Am J Hematol 1985; 78: 869–872.
11. Montefusco E, Alimena G, Gastaldi R, Carlesimo OA, Valesini G, Mandelli F. Unusual dermatologic toxicity of long-term therapy with hydroxyurea in chronic myelogenous leukaemia. Tumori 1986; 72: 317–321.
12. Kato N, Kimura K, Yasukawa K, Yoshida K. Hydroxyurea-related leg ulcers in a patient with chronic myelogenous leukemia: a case report and review of the literature. J Dermatol 1999; 26: 56–62.
13. Sirieix ME, Debure C, Baudot N, Dubertret L, Roux ME, Morel P, et al. Leg ulcers and hydroxyurea: forty-one cases. Arch Dermatol 1999; 135: 818–820.
14. Chaine B, Neonato MG, Girot R, Aractingi S. Cutaneous adverse reactions to hydroxyurea in patients with sickle cell disease. Arch Dermatol 2001; 137: 467–470.
15. Saravu K, Velappan P, Lakshmi N, Shastry BA, Thomas J. Hydroxyurea induced perimalleolar ulcers. J Korean Med Sci 2006; 21: 177–179.